

# Reaction of $[\text{Os}_3(\mu\text{-H})_2(\text{CO})_9(\mu_3\text{-CNC}_5\text{H}_4\text{CH=CH}_2)]$ with Phenylacetylene. A Novel Type of Alkylidyne-Alkyne Coupling in a Triosmium Alkylidyne Cluster†

Wai-Yeung Wong, Suzanna Chan and Wing-Tak Wong\*

Department of Chemistry, The University of Hong Kong, Pokfulam Road, Hong Kong

Reaction of the alkylidyne cluster  $[\text{Os}_3(\mu\text{-H})_2(\text{CO})_9(\mu_3\text{-CNC}_5\text{H}_4\text{CH=CH}_2)]$  **1** with the unsymmetrical alkyne  $\text{PhC}\equiv\text{CH}$  occurred under thermal conditions affording two pairs of geometrical isomers  $[\text{Os}_3(\mu\text{-H})(\text{CO})_9\{\mu_3\text{-}\eta^3\text{-PhCCHC(CH=CHPh)}\}]$  **2a** (30%),  $[\text{Os}_3(\text{CO})_9\{\mu_3\text{-}\eta^1\text{-}\eta^2\text{-}\eta^2\text{-}\eta^1\text{-PhCHCH=CH-CH=CPh}\}]$  **2b** (24%),  $[\text{Os}_3(\text{CO})_7\{\mu\text{-}\eta^2\text{-}\eta^2\text{-CH}_2\text{=CHC(Ph)CHCPh}\}\{\mu_3\text{-}\eta^2\text{-C(O)C(Ph)=CH}\}]$  **3a** (8%),  $[\text{Os}_3(\text{CO})_7\{\mu\text{-}\eta^2\text{-}\eta^3\text{-PhCH=CHC(Ph)CHCH}\}\{\mu_3\text{-}\eta^2\text{-C(O)C(Ph)=CH}\}]$  **3b** (6%) and the known cluster  $[\text{Os}_3(\mu\text{-H})(\text{CO})_9\{\mu\text{-C(H)NC}_5\text{H}_4(\eta^2\text{-CH=CH}_2)\}]$  **4** (7%). The same reaction, carried out at room temperature in acetone, yielded another new cluster  $[\text{Os}_3(\text{CO})_9(\mu\text{-}\eta^2\text{-PhCCH}_2)(\mu_3\text{-}\eta^3\text{-CHCPhCH})]$  **5** as a major product (34%). All the compounds have been fully characterised by spectroscopic and X-ray diffraction methods. The structure of **2a** reveals that the methylidyne carbon in the 'Os<sub>3</sub>C' core couples with two phenylacetylene molecules to form a novel C<sub>6</sub> hydrocarbyl co-ordinated in an allyl fashion on the trimetallic surface. Cluster **2b**, an isomer of **2a**, contains a *cis,cis*-1,5-diphenylpenta-1,3-diene ligand on a triangular array of Os atoms which, together with one of the osmium atoms forms an osmacyclohexa-2,4-diene ring with two localised double bonds. The structures of both **3a** and **3b** show the coupling of three alkyne molecules with **1**, resulting in the formation of two discrete organic fragments. An interesting feature in both compounds is the formation of a keto ligand with a  $\mu_3\text{-}\eta^2$ -co-ordination mode, which is derived from the coupling of one carbonyl ligand and a phenylacetylene molecule. The other fragment adopts a  $\mu\text{-}\eta^2\text{-}\eta^3$ -co-ordination mode with a  $\pi$  and a  $\eta^3$ -allyl bond to give a metallacyclic ring system. The two complexes are isomeric and differ only in the spatial positions of the phenyl substituents in the C<sub>6</sub> hydrocarbyl fragments. The structure of **5** contains a  $\sigma,\pi$ -vinyl group with a  $\mu\text{-}\eta^2$ -bonding mode and an allyl fragment with a  $\mu_3\text{-}\eta^3$ -co-ordination mode. A proposed mechanism which involves the cleavage of the N-C(alkylidyne) bond in **1**, resulting in the formation of a  $\mu_3$ -carbido species ' $[\text{Os}_3(\mu\text{-H})_2(\text{CO})_9(\mu_3\text{-C})]$ ' or a  $\mu$ -alkylidene fragment ' $[\text{Os}_3(\mu\text{-H})(\text{CO})_9(\mu\text{-CH})]$ ' as the intermediate is put forward to explain the unusual coupling reaction sequence. The reaction of **1** with *p*-tolylacetylene in refluxing *n*-hexane was studied to support the suggested mechanism and another two pairs of geometrical isomers were fully characterised with the crystal structure of  $[\text{Os}_3(\text{CO})_9(\mu_3\text{-}\eta^1\text{-}\eta^2\text{-}\eta^2\text{-}\eta^1\text{-MeC}_6\text{H}_4\text{CHCH=CHCH=CC}_6\text{H}_4\text{Me})]$  **6b** determined. The basic hydrocarbyl skeleton on the Os<sub>3</sub> triangle in **6b** is essentially the same as in the analogous compound **2b** except for the presence of two methyl groups on the phenyl rings. This precludes the existence of the original pyridine ring in the newly formed clusters.

The chemical reactivities of transition-metal carbonyl clusters containing alkylidene or alkylidyne fragments with unsaturated hydrocarbons are of considerable current interest due to their great potential for generating new and unusual types of linked hydrocarbyl chains and rings.<sup>1</sup> Such reactions usually lead to metal clusters which may be good models of the intermediate surface states in related processes occurring on metal surfaces.<sup>2,3</sup> This is exemplified by the well known methylene coupling as a mechanism of carbon chain growth in the metal-catalysed Fischer-Tropsch reactions.<sup>4</sup> In these reactions, the organometallic clusters promote alkyne oligomerisation and exert a template effect on the resulting organic moieties. These ideas have also produced enormous excitement in the field of alkyne cluster chemistry where an alternative route for large alkyne polymers may be accessed.<sup>5</sup>

We have previously reported the synthesis and crystal structure of the alkylidyne carbonyl cluster  $[\text{Os}_3(\mu\text{-H})_2(\text{CO})_9(\mu_3\text{-CNC}_5\text{H}_4\text{CH=CH}_2)]$  **1**.<sup>6</sup> Its thermal reactivity has been investigated, affording a triosmium alkylidene carbonyl cluster  $[\text{Os}_3(\mu\text{-H})(\text{CO})_9\{\mu\text{-C(H)NC}_5\text{H}_4(\eta^2\text{-CH=CH}_2)\}]$  which

undergoes metal-carbon bond cleavage.<sup>6</sup> These results prompted us to investigate the possibility of alkylidyne-alkyne coupling on such a triosmium cluster and search for a new model for Fischer-Tropsch chain growth.

We describe here the results concerning the reaction of  $[\text{Os}_3(\mu\text{-H})_2(\text{CO})_9(\mu_3\text{-CNC}_5\text{H}_4\text{CH=CH}_2)]$  **1** with phenylacetylene under both ambient and refluxing conditions. Of special importance is the formation of two pairs of geometrical isomers having completely different bonding modes which are obtained by the unprecedented coupling of alkyne molecules to an uncharacterised  $\mu_3$ -carbido species or a  $\mu$ -alkylidene CH fragment after the facile dissociation of the 2-vinylpyridine group in **1**.

## Results and Discussion

Reaction of transition-metal alkylidyne clusters with alkynes usually proceeds non-selectively under more forcing conditions affording a wide range of products frequently in low yields. These involve those arising from C-H activation,<sup>7</sup> C-C coupling,<sup>8</sup> C-C bond cleavage,<sup>9,10</sup> CO activation,<sup>11</sup> hydrogen migration<sup>12,13</sup> as well as isomerisation.<sup>14</sup> Our current investigations show that reaction of the triosmium alkylidyne cluster  $[\text{Os}_3(\mu\text{-H})_2(\text{CO})_9(\mu_3\text{-CNC}_5\text{H}_4\text{CH=CH}_2)]$  **1** with phenyl-

† Supplementary data available: see Instructions for Authors, *J. Chem. Soc., Dalton Trans.*, 1995, Issue 1, pp. xxv-xxx.

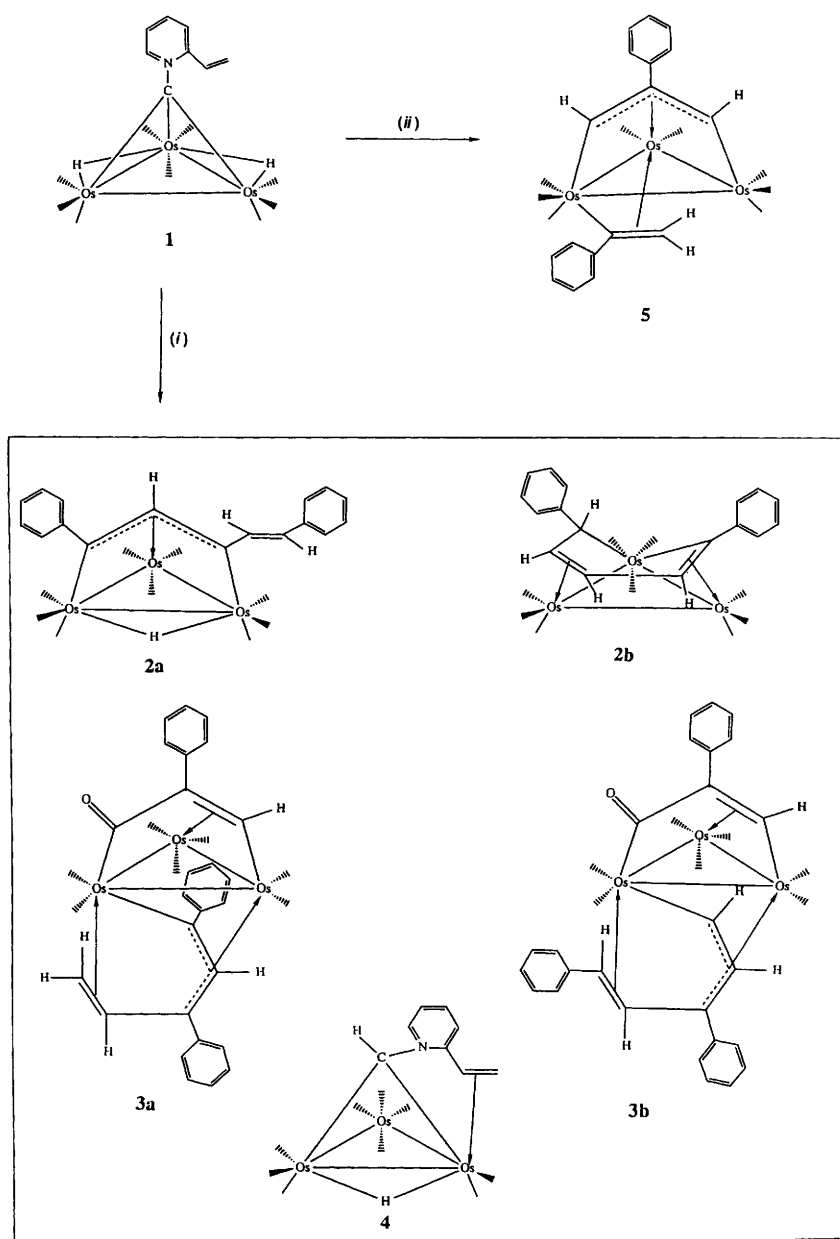
acetylene proceeds under refluxing conditions to afford five products and results in a new reaction sequence of alkylidene-alkyne coupling.

Treatment of **1** with phenylacetylene in refluxing *n*-hexane solution generates two pairs of separable isomers  $[\text{Os}_3(\mu\text{-H})(\text{CO})_9\{\mu_3\text{-}\eta^3\text{-PhCCHC}(\text{CH}=\text{CHPh})\}]$  **2a**,  $[\text{Os}_3(\text{CO})_9(\mu_3\text{-}\eta^1, \eta^2, \eta^2, \eta^1\text{-PhCHCH}=\text{CHCH}=\text{CPh})]$  **2b**,  $[\text{Os}_3(\text{CO})_7\{\mu\text{-}\eta^2, \eta^3\text{-CH}_2=\text{CHC}(\text{Ph})\text{CHCPh}\}\{\mu_3\text{-}\eta^2\text{-C}(\text{O})\text{C}(\text{Ph})=\text{CH}\}]$  **3a** and  $[\text{Os}_3(\text{CO})_7\{\mu\text{-}\eta^2, \eta^3\text{-PhCH}=\text{CHC}(\text{Ph})\text{CHCH}\}\{\mu_3\text{-}\eta^2\text{-C}(\text{O})\text{C}(\text{Ph})=\text{CH}\}]$  **3b** in 30, 24, 8 and 6% yields respectively. A previously reported alkylidene cluster  $[\text{Os}_3(\text{CO})_9(\mu\text{-C}(\text{H})\text{NC}_5\text{H}_4(\eta^2\text{-CH}=\text{CH}_2))]$  **4** was also obtained in 7% yield. However, when the same reaction was performed in acetone at ambient temperature, a major product was isolated and characterised as  $[\text{Os}_3(\text{CO})_8(\mu\text{-}\eta^2\text{-PhCCH}_2)(\mu_3\text{-}\eta^3\text{-CHCPhCH})]$  **5** (34%). The transformations of these products are shown in Scheme 1.

On the basis of identical positive FAB mass spectra as well as elemental analyses, both compounds **2a** and **2b** are probably isomeric. However, spectroscopic (IR and  $^1\text{H}$  NMR) evidence shows that they are completely different (Table 1, Fig. 1).

Crystal structure analyses of both complexes were therefore undertaken in order to establish their molecular geometries and in particular to elucidate the modes of co-ordination of the organic ligands to the metal clusters.

A perspective view of the molecular structure of complex **2a** together with the atomic numbering scheme is illustrated in Fig. 2. Table 2 contains selected interatomic distances and angles. The cluster **2a** is electron precise and contains a total of 48 cluster valence electrons. The molecular structure reveals that C-C bond formation has occurred by thermally induced coupling, linking two alkynes and the methylidyne carbon in the 'Os<sub>3</sub>C' core together. The 2-vinylpyridine group is dissociated from **1** during the reaction. The resulting organic fragment is bonded to the triosmium unit in a  $\mu_3\text{-}\eta^3$  fashion, formally *via* a  $\pi$ - and two  $\sigma$ -allyl bonds. In this bonding mode, the organic ligand acts as a five-electron donor and contains a central C<sub>3</sub> unit associated with the metal core.<sup>14</sup> The hydrocarbyl fragment can be considered as a *trans*-1,5-diphenylpent-1-ene ligand located directly over the metal triangle. The unco-ordinated alkene unit adopts a *trans* conformation. We believe the cluster-bound hydride of **1** is



Scheme 1 (i) PhCCH, *n*-hexane, reflux; (ii) PhCCH, acetone, room temperature

**Table 1** Spectroscopic data for compounds **2a**, **2b**, **3a**, **3b**, **5**, **6a**, **6b**, **7a** and **7b**

Compound	IR $\tilde{\nu}(\text{CO})/\text{cm}^{-1}$	$^1\text{H NMR } \delta^a$	MS (m/z) <sup>b</sup>
<b>2a</b> (R = H)	2097s, 2071vs, 2049vs, 2021vs, 2008 (sh), 2003vs, 1987m <sup>c</sup>	8.54 [d, 1 H, $J(\text{H}_c\text{H}_d)$ 1.7, H <sub>c</sub> ] 7.44 (m, 10 H, phenyl) 7.29 [d, 1 H, $J(\text{H}_a\text{H}_b)$ 15.6, H <sub>a</sub> or H <sub>b</sub> ] 7.10 [d, 1 H, $J(\text{H}_a\text{H}_b)$ 15.6, H <sub>a</sub> or H <sub>b</sub> ] - 18.56 [d, 1 H, $J(\text{H}_d\text{H}_e)$ 1.7, H <sub>d</sub> ]	1046 (1046)
<b>2b</b>	2085vs, 2071m, 2051vs, 2038vs, 2015vs, 1998s, 1980m, 1971s <sup>c</sup>	7.37 (m, 5 H, phenyl) 7.15 (m, 5 H, phenyl) 6.64 (d, 1 H, $J$ 4.2) 4.89 (dt, 1 H, $J$ 1.2, 4.2 and 5.6) 4.62 (dd, 1 H, $J$ 5.6 and 3.9) 3.54 (dd, 1 H, $J$ 3.9 and 1.2)	1046 (1046)
<b>3a</b> (R = H)	2082s, 2054m, 2029vs, 2009s, 1978w, 1725w (br) <sup>d</sup>	9.46 (s, 1 H, H <sub>e</sub> ) 7.45 (m, 14 H, phenyl) 7.00 [m, 2 H, H <sub>d</sub> + 1 H (phenyl)] 6.02 [d, 1 H, $J(\text{H}_c\text{H}_d)$ 1.7, H <sub>c</sub> ] 2.46 [d, 1 H, $J(\text{H}_a\text{H}_d)$ 12.0, H <sub>a</sub> ] 2.28 [d, 1 H, $J(\text{H}_b\text{H}_d)$ 7.6, H <sub>b</sub> ]	1120 (1120)
<b>3b</b> (R = H)	2083s, 2044s, 2023vs, 2010 (sh), 1971w, 1964w, 1726w (br) <sup>d</sup>	9.53 (s, 1 H, H <sub>e</sub> ) 8.90 [d, 1 H, $J(\text{H}_d\text{H}_e)$ 5.6, H <sub>d</sub> ] 7.37 (m, 15 H, phenyl) 6.48 [dd, 1 H, $J(\text{H}_c\text{H}_b)$ 1.5, $J(\text{H}_c\text{H}_d)$ 5.6, H <sub>c</sub> ] 5.63 [dd, 1 H, $J(\text{H}_b\text{H}_a)$ 12.2, $J(\text{H}_b\text{H}_c)$ 1.5, H <sub>b</sub> ] 4.28 [d, 1 H, $J(\text{H}_a\text{H}_b)$ 12.2, H <sub>a</sub> ]	1120 (1120)
<b>5</b>	2084s, 2054vs, 2022vs, 2006vs, 1987m, 1978w, 1767m <sup>c</sup>	9.42 (d, 1 H, $J$ 2.3) 7.64 (m, 5 H, phenyl) 7.42 (m, 5 H, phenyl) 6.11 (d, 1 H, $J$ 2.3) 4.26 (d, 1 H, $J$ 1.7) 3.95 (d, 1 H, $J$ 1.7)	1018 (1018)
<b>6a</b> (R = Me)	2096s, 2070vs, 2048vs, 2019vs, 2007 (sh), 2002vs, 1986m <sup>c</sup>	8.53 [d, 1 H, $J(\text{H}_c\text{H}_d)$ 1.5, H <sub>c</sub> ] 7.29 (m, 8 H, C <sub>6</sub> H <sub>4</sub> ) 7.25 [d, 1 H, $J(\text{H}_a\text{H}_b)$ 15.4, H <sub>a</sub> or H <sub>b</sub> ] 7.08 [d, 1 H, $J(\text{H}_a\text{H}_b)$ 15.4, H <sub>a</sub> or H <sub>b</sub> ] 2.38 (s, 3 H, Me) 2.33 (s, 3 H, Me) - 18.57 [d, 1 H, $J(\text{H}_d\text{H}_e)$ 1.5, H <sub>d</sub> ]	1074 (1074)
<b>6b</b>	2084vs, 2069m, 2050vs, 2036vs, 2014vs, 1996s, 1979m, 1970s <sup>c</sup>	7.23 (m, 8 H, C <sub>6</sub> H <sub>4</sub> ) 6.60 (d, 1 H, $J$ 4.2) 4.86 (dt, 1 H, $J$ 1.2, 4.2 and 5.8) 4.59 (dd, 1 H, $J$ 5.8 and 3.9) 3.49 (dd, 1 H, $J$ 3.9 and 1.2) 2.35 (s, 3 H, Me) 2.27 (s, 3 H, Me)	1074 (1074)
<b>7a</b> (R = Me)	2079s, 2050s, 2026vs, 2006s, 1975w, 1726w (br) <sup>d</sup>	9.39 (s, 1 H, H <sub>e</sub> ) 7.33 (m, 11 H, C <sub>6</sub> H <sub>4</sub> ) 6.89 [m, 2 H, H <sub>a</sub> + 1 H (phenyl)] 5.94 [d, 1 H, $J(\text{H}_c\text{H}_d)$ 1.5, H <sub>c</sub> ] 2.43 [d, 1 H, $J(\text{H}_a\text{H}_d)$ 12.0, H <sub>a</sub> ] 2.39 (s, 6 H, 2 Me) 2.24 (s, 3 H, Me)	1162 (1162)
<b>7b</b> (R = Me)	2081s, 2041s, 2022vs, 2010 (sh), 1969w, 1963w, 1725w (br) <sup>d</sup>	2.23 [d, 1 H, $J(\text{H}_b\text{H}_d)$ 7.6, H <sub>b</sub> ] 9.47 (s, 1 H, H <sub>e</sub> ) 8.87 [d, 1 H, $J(\text{H}_d\text{H}_e)$ 5.1, H <sub>d</sub> ] 7.16 (m, 12 H, C <sub>6</sub> H <sub>4</sub> ) 6.40 [dd, 1 H, $J(\text{H}_c\text{H}_b)$ 1.2, $J(\text{H}_c\text{H}_d)$ 5.1, H <sub>c</sub> ] 5.58 [dd, 1 H, $J(\text{H}_b\text{H}_a)$ 12.2, $J(\text{H}_b\text{H}_c)$ 1.2, H <sub>b</sub> ] 4.29 [d, 1 H, $J(\text{H}_a\text{H}_b)$ 12.2, H <sub>a</sub> ] 2.41 (s, 3 H, Me) 2.36 (s, 3 H, Me) 2.34 (s, 3 H, Me)	1162 (1162)

<sup>a</sup> In CD<sub>2</sub>Cl<sub>2</sub>,  $J$  values in Hz. <sup>b</sup> Based on <sup>192</sup>Os. <sup>c</sup> In *n*-hexane. <sup>d</sup> In CH<sub>2</sub>Cl<sub>2</sub>.

probably the source of the hydrogen atom on the vinyl group. The carbon atom C(12), presumed to be the original alkylidyne carbon in **1**, is bound to carbon atom C(13) of a phenylacetylene molecule, which together with C(14) forms a  $\pi$ -allyl bond to Os(1).

The structure of complex **2a** defines an irregular metal triangle with the Os(2)–Os(3) bond [2.952(1) Å] being significantly longer than the other two [Os(1)–Os(2) 2.812(1), Os(1)–Os(3) 2.823(1) Å]. Such a long bond distance between

Os(2) and Os(3) is indicative of the presence of a hydride atom spanning this edge, which is also consistent with the potential energy calculations.<sup>15</sup> The allyl moiety is  $\sigma$  bonded to Os(3) [Os(3)–C(12) 2.08(1) Å] and to Os(2) [Os(2)–C(14) 2.10(1) Å]. It is also bonded in an  $\eta^3$  fashion to Os(1) [Os(1)–C(12) 2.33(1), Os(1)–C(13) 2.27(1), Os(1)–C(14) 2.34(1) Å]. The carbon–carbon distances within the  $\eta^3$ -allyl system are C(12)–C(13) 1.44(3) and C(13)–C(14) 1.42(3) Å [av. 1.43(3) Å]. The C(10)–C(11) distance [1.34(2) Å] is consistent with the

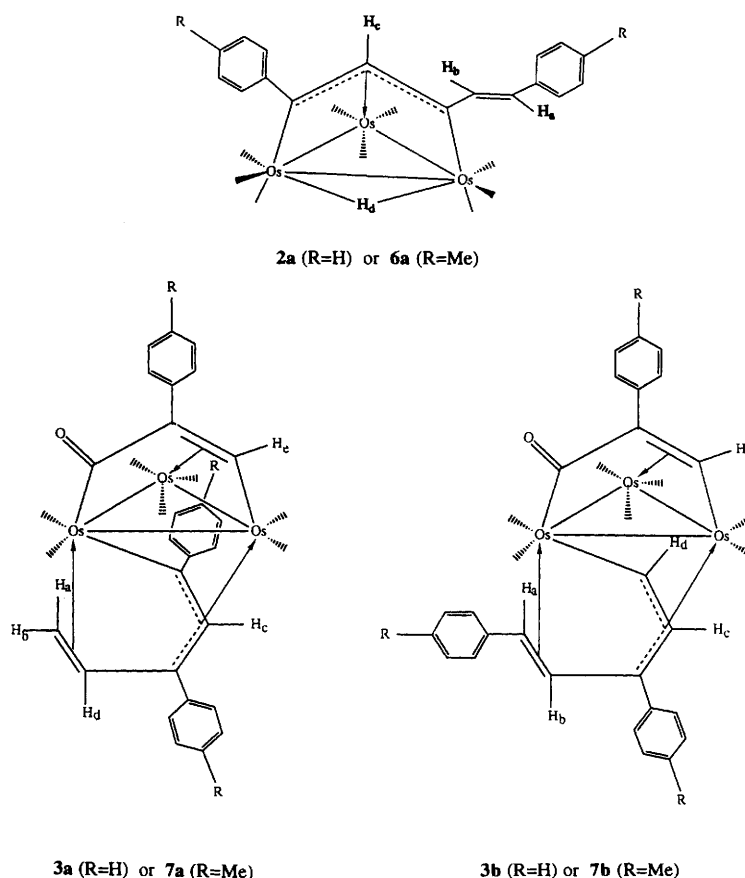


Fig. 1 Labelling schemes used for the assignments of  $^1\text{H}$  NMR spectra

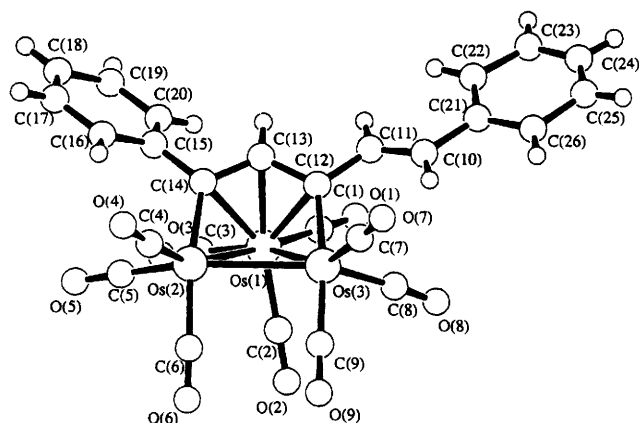


Fig. 2 Molecular structure of complex **2a**, showing the atomic labelling scheme

observation that it shows no interaction with the osmium atom(s). The other distances within the organic ligand are internally consistent.

The spectroscopic data for complex **2a** are fully consistent with the solid-state structure (Table 1, Fig. 1). The positive FAB mass spectrum of **2a** shows an envelope with a molecular ion peak at 1046. The  $^1\text{H}$  NMR spectrum of **2a** in  $\text{CD}_2\text{Cl}_2$  shows a doublet at  $\delta - 18.56$  with  $J_{(\text{HH})}$  1.7 Hz which indicates the presence of a metal hydride. It was shown, by spin-decoupling experiments, to be long-range coupled with the doublet centred at  $\delta 8.54$ , assigned as the proton on C(13). The IR data of **2a** show close resemblance to those of clusters of the type  $[\text{M}_3(\mu\text{-H})(\text{CO})_9(\mu_3\text{-}\eta^3\text{-RCCR'CR'')}]$  ( $\text{M} = \text{Os}$  or  $\text{Ru}$ )<sup>16,17</sup> which contain similar face-bonded ( $2\sigma + \pi$ )-allyl ligands. The structure of **2a** shows that the  $\text{Os}_3\text{C}_3$  framework may be described as a *nido* polyhedron based upon a pentagonal bipyramid.<sup>18</sup>

Table 2 Selected bond distances ( $\text{\AA}$ ) and angles ( $^\circ$ ) for complex **2a**

Os(1)–Os(2)	2.812(1)	Os(2)–Os(3)	2.952(1)
Os(1)–Os(3)	2.823(1)	Os(1)–C(12)	2.33(1)
Os(1)–C(13)	2.27(1)	Os(1)–C(14)	2.34(1)
Os(2)–C(14)	2.10(1)	Os(3)–C(12)	2.08(1)
C(10)–C(11)	1.34(2)	C(11)–C(12)	1.50(2)
C(12)–C(13)	1.44(3)	C(13)–C(14)	1.42(3)
C(10)–C(21)	1.51(3)	C(14)–C(15)	1.49(2)
Os(2)–Os(1)–Os(3)	63.18(2)	Os(1)–Os(2)–Os(3)	58.60(3)
Os(1)–Os(3)–Os(2)	58.21(3)	Os(1)–Os(2)–C(14)	54.7(4)
Os(1)–Os(3)–C(12)	53.9(4)	Os(2)–Os(1)–C(12)	83.2(4)
Os(2)–Os(1)–C(13)	74.5(4)	Os(2)–Os(1)–C(14)	46.9(4)
Os(3)–Os(1)–C(12)	46.5(4)	Os(3)–Os(1)–C(13)	74.7(4)
Os(3)–Os(1)–C(14)	83.4(4)	C(12)–Os(1)–C(14)	65.8(6)
Os(2)–C(14)–C(13)	124(2)	Os(3)–C(12)–C(13)	124(7)
C(11)–C(10)–C(21)	124(2)	C(10)–C(11)–C(12)	125(1)
C(11)–C(12)–C(13)	112(1)	C(12)–C(13)–C(14)	124(1)
C(13)–C(14)–C(15)	114(1)		

The molecular structure of complex **2b** has also been established by X-ray crystallography and is depicted in Fig. 3, together with the atomic numbering scheme. Selected interatomic distances and angles are given in Table 3. The three osmium atoms also define an irregular triangle with the Os(1)–Os(3) distance [2.807(2)  $\text{\AA}$ ] being the shortest. This edge is significantly shorter than the Os–Os distance of 2.877(3)  $\text{\AA}$  in the parent binary carbonyl  $[\text{Os}_3(\text{CO})_{12}]$ .<sup>19</sup> The molecular structure of **2b** shows that a novel  $\text{C}_5\text{Os}_3$  unit is produced where two incoming phenylacetylene molecules are fused together with the apical carbon to form an interesting *cis,cis*-1,5-diphenylpenta-1,3-diene moiety.<sup>20</sup> Strong  $\sigma$ -bonding interactions exist between Os(2) and C(10) as well as C(14). Hence, the organic ligand together with Os(2) forms an osma-

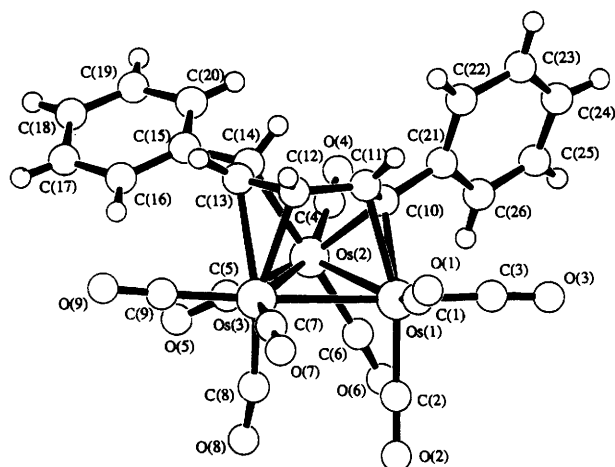


Fig. 3 Molecular structure of complex **2b**, showing the atomic labelling scheme

Table 3 Selected bond distances (Å) and angles (°) for complex **2b**

Os(1)–Os(2)	2.852(1)	Os(2)–Os(3)	2.845(1)
Os(1)–Os(3)	2.807(2)	Os(1)–C(10)	2.19(2)
Os(1)–C(11)	2.33(2)	Os(2)–C(10)	2.17(2)
Os(2)–C(14)	2.29(2)	Os(3)–C(12)	2.27(2)
Os(3)–C(13)	2.41(2)	C(10)–C(11)	1.41(3)
C(11)–C(12)	1.51(4)	C(12)–C(13)	1.40(4)
C(13)–C(14)	1.44(3)	C(14)–C(15)	1.52(4)
C(10)–C(21)	1.52(3)		
Os(2)–Os(1)–Os(3)	60.35(3)	Os(1)–Os(2)–Os(3)	59.04(3)
Os(1)–Os(3)–Os(2)	60.61(3)	Os(1)–Os(2)–C(10)	49.5(6)
Os(1)–Os(2)–C(14)	108.1(6)	Os(2)–Os(1)–C(10)	48.8(6)
Os(2)–Os(1)–C(11)	70.9(6)	Os(2)–Os(3)–C(12)	77.3(6)
Os(2)–Os(3)–C(13)	68.0(6)	Os(3)–Os(2)–C(10)	86.7(6)
Os(3)–Os(2)–C(14)	76.1(6)	Os(1)–C(11)–C(10)	66(1)
Os(2)–C(10)–C(11)	115(2)	Os(2)–C(14)–C(13)	103(2)
Os(3)–C(13)–C(14)	110(2)	C(10)–Os(2)–C(14)	77.3(9)
C(10)–C(11)–C(12)	122(2)	C(11)–C(12)–C(13)	122(2)
C(12)–C(13)–C(14)	119(2)	C(13)–C(14)–C(15)	115(2)
C(11)–C(10)–C(21)	120(2)		

cyclohexadiene ring. Although there are numerous examples of metal cluster complexes containing metallacyclopentadiene rings,<sup>21</sup> metallacyclohexadienyl cluster complexes are rare. Nevertheless, such a mode of co-ordination has been observed in  $[\text{Os}_3(\text{CO})_9\{\text{EtC}_2\text{H}_2\text{CO}\}]$ .<sup>22</sup> The C(10)–C(11)–C(12)–C(13)–C(14) fragment in **2b** essentially defines a cisoid 1,3-diene with the interior angles roughly equal to 120°. The substituted pentanuclear chain is characterised by the localisation of the two double bonds, as shown by the C–C bond distances [C(10)–C(11) 1.41(3) and C(12)–C(13) 1.40(4) Å]. This fragment forms two separate  $\pi$  bonds to Os(1) and Os(3). The C(11)–C(12) bond is formally a single bond [1.51(4) Å].<sup>23</sup> This is in contrast to the extensive delocalisation observed in mononuclear complexes in which the ligand is co-ordinated to the metal centre in an  $\eta^5$  fashion.<sup>24</sup> The resulting organic moiety is therefore co-ordinated to the trimetallic cluster *via* two  $\sigma$  and two  $\pi$  bonds. In total, the ligand donates six electrons to the cluster and each osmium atom obeys the 18-electron rule. As in **2a**, C(12) is probably the original alkyldiene carbon in **1** and is coupled to C(11) and C(13) of the two phenylacetylene molecules. Hydride migration also occurs in **2b** to provide two hydrogen atoms for the ligand. The molecule is formally derived from  $[\text{Os}_3(\text{CO})_{12}]$  by replacing three terminal CO ligands by a six-electron donating  $\mu_3\text{-}\eta^1, \eta^2, \eta^2, \eta^1\text{-PhCH=CH=CH=CH=CPh}$  ligand. A similar situation has recently been observed in a triosmium carbonyl cluster with a carbene ligand co-ordinated in an unusual  $\mu_3\text{-}\eta^2, \eta^2, \eta^2$  face-capping bonding

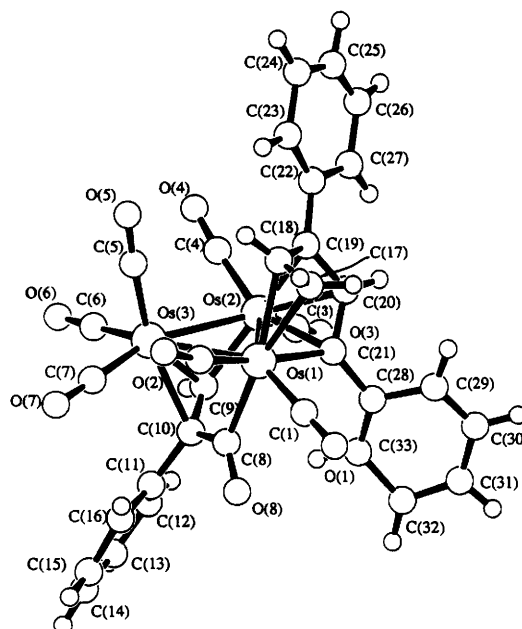


Fig. 4 Molecular structure of complex **3a**, showing the atomic labelling scheme

mode.<sup>25</sup> Of special interest is the potential capability of generating  $\pi$ -hydrocarbon rings. Such metal cluster-induced organic transformations may provide a novel route to the cyclisation of organic molecules, which is often inaccessible by conventional strategies.<sup>26,27</sup>

With the aid of the solid-state structure of **2b**, it is now possible to interpret its  $^1\text{H}$  NMR spectrum, which shows a rather complex pattern (Table 1). Multiplets due to the 10 phenyl protons were observed in the range  $\delta$  7.15–7.37. The resonances were assigned with the aid of two-dimensional NMR experiments. The proton at  $\delta$  4.89 is spin-coupled to the other three protons simultaneously to give a doublet of triplets with three different coupling constants,  $J(\text{HH})$  1.2, 4.2 and 5.6 Hz. The signal at  $\delta$  6.64 appears as a doublet with  $J(\text{HH})$  4.2 Hz, which is only coupled to the proton at  $\delta$  4.89. Resonances at  $\delta$  3.54 and 4.62 are spin-coupled to each other with  $J(\text{HH})$  3.9 Hz, which, by another coupling with the proton at  $\delta$  4.89 with  $J(\text{HH})$  1.2 and 5.6 Hz respectively, give rise to two sets of doublets of doublets. However, no attempt has been made to assign fully the actual positions of these four protons. The positive FAB mass spectrum of **2b** also shows a molecular ion peak at 1046.

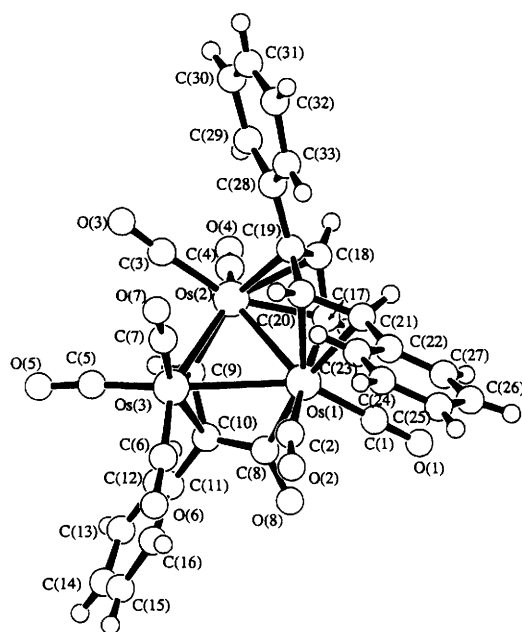
A single red product was obtained after preparative TLC following the thermolytic reaction of **1** with  $\text{PhC}\equiv\text{CH}$ . However, careful separation by repeated TLC led to two isomeric red products, **3a** and **3b**, in low yields (8 and 6% respectively). These products possess completely different  $^1\text{H}$  NMR spectral patterns (Table 1, Fig. 1), yet identical molecular ion peaks at 1120 are observed in their mass spectra. Crystal structure analyses of **3a** and **3b** were therefore carried out in order to establish unequivocally the exact nature of the bonding of the hydrocarbyl fragments to the cluster framework. The molecular structure of complex **3a** is illustrated in Fig. 4, together with the atomic numbering scheme. The important bond distances and angles are given in Table 4. The cluster **3a** is electron precise. The molecular structure reveals that coupling of three alkyne molecules with **1** occurs which gives rise to two discrete hydrocarbyl ligands. A salient structural feature is the direct coupling of one terminal carbonyl group and a phenylacetylene molecule.<sup>22,28</sup> This is evident from the IR spectrum which displays a band at  $1725\text{ cm}^{-1}$  due to the ketonic carbonyl ligand. This resulting ligand is co-ordinated in a  $\mu_3\text{-}\eta^2$  fashion to the  $\text{Os}_3$  triangle, formally *via* a  $\pi$  and two  $\sigma$  bonds and acts as a four-electron donor. Another fragment, derived

**Table 4** Selected bond distances (Å) and angles (°) for complex **3a**

Os(1)–Os(2)	2.756(2)	Os(2)–Os(3)	2.742(2)
Os(1)–Os(3)	2.858(2)	Os(1)–C(8)	2.15(3)
Os(1)–C(17)	2.34(3)	Os(1)–C(18)	2.27(3)
Os(1)–C(21)	2.14(2)	Os(2)–C(9)	2.07(3)
Os(2)–C(19)	2.32(2)	Os(2)–C(20)	2.21(2)
Os(2)–C(21)	2.20(2)	Os(3)–C(9)	2.22(2)
Os(3)–C(10)	2.35(3)	C(8)–C(10)	1.48(4)
C(9)–C(10)	1.36(3)	C(10)–C(11)	1.53(4)
C(17)–C(18)	1.34(3)	C(18)–C(19)	1.52(3)
C(19)–C(20)	1.42(3)	C(20)–C(21)	1.42(3)
C(19)–C(22)	1.48(3)	C(21)–C(28)	1.46(3)
C(8)–O(8)	1.21(3)		
Os(2)–Os(1)–Os(3)	58.45(4)	Os(1)–Os(2)–Os(3)	62.64(4)
Os(1)–Os(3)–Os(2)	58.92(4)	Os(1)–Os(2)–C(19)	72.1(6)
Os(1)–Os(2)–C(20)	73.4(6)	Os(1)–Os(2)–C(21)	49.7(6)
Os(1)–Os(3)–C(9)	79.4(6)	Os(1)–Os(3)–C(10)	71.2(7)
Os(2)–Os(1)–C(17)	101.3(7)	Os(2)–Os(1)–C(18)	72.8(6)
Os(2)–Os(1)–C(21)	51.6(6)	Os(2)–Os(3)–C(9)	47.8(6)
Os(2)–Os(3)–C(10)	73.4(7)	Os(3)–Os(2)–C(19)	107.7(6)
Os(3)–Os(2)–C(20)	131.9(6)	Os(1)–C(8)–C(10)	113(2)
Os(1)–C(21)–C(20)	113(1)	Os(2)–C(9)–C(10)	124(1)
Os(2)–C(20)–C(21)	71(1)	Os(2)–C(21)–C(20)	71(1)
C(17)–Os(1)–C(21)	82.2(9)	C(18)–Os(1)–C(21)	78.4(9)
C(8)–C(10)–C(9)	122(2)	C(9)–C(10)–C(11)	122(2)
C(17)–C(18)–C(19)	122(2)	C(18)–C(19)–C(20)	113(2)
C(19)–C(20)–C(21)	117(2)		

**Table 5** Selected bond distances (Å) and angles (°) for complex **3b**

Os(1)–Os(2)	2.746(2)	Os(2)–Os(3)	2.729(2)
Os(1)–Os(3)	2.871(2)	Os(1)–C(8)	2.10(3)
Os(1)–C(17)	2.06(3)	Os(1)–C(20)	2.29(4)
Os(1)–C(21)	2.35(4)	Os(2)–C(9)	1.98(3)
Os(2)–C(17)	2.12(3)	Os(2)–C(18)	2.15(4)
Os(2)–C(19)	2.27(4)	Os(3)–C(9)	2.23(3)
Os(3)–C(10)	2.33(3)	C(8)–C(10)	1.43(4)
C(9)–C(10)	1.46(4)	C(10)–C(11)	1.51(4)
C(17)–C(18)	1.44(4)	C(18)–C(19)	1.30(5)
C(19)–C(20)	1.46(5)	C(19)–C(28)	1.56(5)
C(20)–C(21)	1.45(5)	C(21)–C(22)	1.56(5)
C(8)–O(8)	1.25(3)		
Os(2)–Os(1)–Os(3)	58.09(5)	Os(1)–Os(2)–Os(3)	63.25(5)
Os(1)–Os(3)–Os(2)	58.66(5)	Os(1)–Os(2)–C(17)	48.1(8)
Os(1)–Os(2)–C(18)	72.8(9)	Os(1)–Os(2)–C(19)	71.0(10)
Os(1)–Os(3)–C(9)	76.9(7)	Os(1)–Os(3)–C(10)	70.8(7)
Os(2)–Os(1)–C(20)	71.9(10)	Os(2)–Os(1)–C(21)	101.0(8)
Os(2)–Os(3)–C(9)	45.8(8)	Os(2)–Os(3)–C(10)	75.4(7)
Os(3)–Os(1)–C(20)	90.0(10)	Os(3)–Os(1)–C(21)	124.2(8)
Os(3)–Os(2)–C(17)	110.5(8)	Os(3)–Os(2)–C(18)	130.1(9)
Os(3)–Os(2)–C(19)	105.8(10)	Os(1)–C(8)–C(10)	117(2)
Os(1)–Os(3)–C(18)	113(2)	C(8)–C(10)–C(9)	116(2)
C(17)–C(18)–C(19)	116(3)	C(18)–C(19)–C(20)	118(3)
C(19)–C(20)–C(21)	116(3)		

**Fig. 5** Molecular structure of complex **3b**, showing the atomic labelling scheme

from the head-to-tail coupling of two phenylacetylene units with the original methylidyne carbon in **1**, acts as a six-electron donor. This organic  $C_5$  unit remains independently coordinated to the osmium triangle from above and below in a  $\mu-\eta^2, \eta^3$  mode to give a metallacyclic ring. This ring is  $\sigma$  bonded to Os(1) through C(21). A  $\pi$ -bonding interaction is also observed from C(17)–C(18) to Os(1) and the fragment C(19)–C(20)–C(21) forms a  $\pi$ -allyl bond to Os(2). It is most likely that C(17) is the original methylidyne carbon in **1** and the formation of **3a** is accompanied by rupture of one N–C(alkylidyne) bond and two Os–C(alkylidyne) bonds in **1**.

Within the triangular osmium framework of **3a**, the edge Os(1)–Os(3) [2.858(2) Å] is significantly longer than the other two [Os(1)–Os(2) 2.756(2) Å, Os(2)–Os(3) 2.742(2) Å]. The structure of **3a** shows the presence of a keto group with

C(8)–O(8) 1.21(3) Å [*cf.* C(7)–O(7) 1.18(3) Å]. The whole  $\mu_3-\eta^2$  fragment forms two  $\sigma$  bonds with Os(1) and Os(2) [Os(1)–C(8) 2.15(3), Os(2)–C(9) 2.07(3) Å] and one  $\pi$  bond with Os(3) [Os(3)–C(9) 2.22(2), Os(3)–C(10) 2.35(3) Å]. The edge C(9)–C(10) is 1.36(3) Å long. The other  $C_5$  unit is bonded to the Os(1)–Os(2) edge *via* a  $\mu-\eta^2, \eta^3$  mode. The distance of the C(17)–C(18) double bond is 1.34(3) Å while the distances within the  $\pi$ -allyl system are C(19)–C(20) 1.42(3) and C(20)–C(21) 1.42(3) Å.

A perspective view of the molecular structure of complex **3b** together with the atomic numbering scheme is illustrated in Fig. 5. The selected bond distances and angles are listed in Table 5. A ketonic carbonyl ligand is also present in **3b**. This is consistent with its solution IR spectrum which shows a band at 1726  $cm^{-1}$ . The metal triangle and the hydrocarbyl ligands are essentially the same as in complex **3a**. The only difference observed lies in the positions of the phenyl substituents in the  $C_5$  hydrocarbyl fragments. The metal Os(1) is involved in an  $\eta^2$  interaction to the fragment C(20)–C(21) [Os(1)–C(20) 2.29(4), Os(1)–C(21) 2.35(4) Å]. Moreover, the fragment C(17)–C(18)–C(19) forms a  $\pi$ -allyl bond to Os(2) with Os(2)–C(17) 2.12(3), Os(2)–C(18) 2.15(4) and Os(2)–C(19) 2.27(4) Å.<sup>29</sup> The distances within the  $\pi$ -allyl system are C(17)–C(18) 1.44(4) and C(18)–C(19) 1.30(5) Å. The isolation of complexes **3a** and **3b** represents the possibility of alkyne oligomerisation and CO functionalisation to give novel hydrocarbyl fragments on triosmium clusters. Hence, this is a further example of the potential of the clusters in the building-up of organic molecules.

The molecular geometry of complex **5** and its atomic labelling is depicted in Fig. 6. The selected interatomic bond distances and angles are given in Table 6. The molecular structure of **5**, an octacarbonyl product, reveals that one molecule of the alkyne has coupled to the exposed carbido site, giving a five-electron donating  $\mu_3-\eta^3$ -CHCPhCH ligand, but that the second molecule has inserted into the osmium–hydride linkage to give a three-electron donating vinyl  $\mu-\eta^2$ -PhCCH<sub>2</sub> unit. Altogether the two organic fragments contribute eight electrons to the cluster unit. A cluster with a similar bonding mode has been encountered in  $[Os_3(CO)_8(\mu-\eta^2-PhCCHPh)(\mu-\eta^3-C_3Ph_3)]$ .<sup>30</sup> The formal electron count on each osmium atom indicates that Os(2) is electron rich (19 electrons), whereas Os(3) is electron deficient (17 electrons). The Os(1) atom is electron precise (18 electrons). The Os–Os distances show substantial differences

compared to the parent cluster  $[\text{Os}_3(\text{CO})_{12}]$  with  $\text{Os}(1)\text{--}\text{Os}(3)$  2.910(1) Å being the longest. The  $\mu\text{-}\eta^2\text{-vinyl}$  ligand is  $\sigma$  bonded to  $\text{Os}(1)$  [ $\text{Os}(1)\text{--}\text{C}(10)$  2.17(4) Å] and  $\pi$  bonded to  $\text{Os}(2)$  [ $\text{Os}(2)\text{--}\text{C}(9)$  2.37(5),  $\text{Os}(2)\text{--}\text{C}(10)$  2.31(4) Å] with  $\text{C}(9)\text{--}\text{C}(10)$  1.49(6) Å. The  $\mu_3\text{-}\eta^3\text{-CHCPhCH}$  fragment is  $\sigma$  bonded to  $\text{Os}(1)$  [ $\text{Os}(1)\text{--}\text{C}(17)$  2.18(3) Å] and to  $\text{Os}(3)$  [ $\text{Os}(3)\text{--}\text{C}(19)$  2.06(4) Å]. It is also bonded in an  $\eta^3$  fashion to  $\text{Os}(2)$  [ $\text{Os}(2)\text{--}\text{C}(17)$  2.15(4),  $\text{Os}(2)\text{--}\text{C}(19)$  2.32(4),  $\text{Os}(2)\text{--}\text{C}(18)$  2.44(3) Å].

The spectroscopic data for complex **5** are fully consistent with the solid-state structure. An intense molecular ion peak at 1018 was observed in the positive FAB mass spectrum. Its  $^1\text{H}$  NMR spectrum shows two sets of multiplets between  $\delta$  7.42 and 7.64 for the 10 phenyl protons. The two terminal methylene protons on  $\text{C}(9)$ , which are magnetically non-equivalent, give rise to two sets of doublets due to geminal coupling. Similarly, the proton on  $\text{C}(17)$  is spin-coupled to that on  $\text{C}(19)$  to give two doublets.

On the basis of the molecular structures of **2a**, **2b**, **3a**, **3b** and **5**, a mechanism is proposed (Scheme 2) for the reaction of **1** with  $\text{PhC}\equiv\text{CH}$ . The initial step involves the facile dissociation of the 2-vinylpyridine group affording the  $\mu_3\text{-carbido}$  species  $[\text{Os}_3(\mu\text{-H})_2(\text{CO})_9(\mu_3\text{-C})]$  or the  $\mu\text{-alkylidene}$  fragment  $[\text{Os}_3(\mu\text{-H})(\text{CO})_9(\mu\text{-CH})]$  as the possible intermediate. The fate of the 2-vinylpyridine after the reaction has been established by  $^1\text{H}$  NMR spectroscopy and it was found that it remains intact in the reaction mixture. Direct coupling between the alkyne(s) and the intermediate occurs and leads to carbon-carbon bond formation of different bonding modes. The identity of the heteroatom is crucial to the reaction mechanism. Satisfactory elemental analyses of the new clusters **2a**, **2b** and **5** were obtained all of which showed the absence of nitrogen, but the extremely poor yields of **3a** and **3b** precluded any satisfactory measurements. Attempts have been made to support the suggested mechanism by studying the analogous reaction of complex **1** with *p*-tolylacetylene in refluxing *n*-hexane. As expected, we obtained a series of analogous compounds, namely, **4**,  $[\text{Os}_3(\mu\text{-H})(\text{CO})_9\{\mu_3\text{-}\eta^3\text{-MeC}_6\text{H}_4\text{CCHCCH}=\text{CH}(\text{C}_6\text{H}_4\text{Me})\}]$  **6a**,  $[\text{Os}_3(\text{CO})_9\{\mu_3\text{-}\eta^1,\eta^2,\eta^2,\eta^1\text{-MeC}_6\text{H}_4\text{CH}=\text{CH}=\text{CHCH}=\text{CC}_6\text{H}_4\text{Me}\}]$  **6b**,  $[\text{Os}_3(\text{CO})_7\{\mu\text{-}\eta^2,\eta^3\text{-CH}_2=\text{CH}(\text{C}_6\text{H}_4\text{Me})\text{CHCC}_6\text{H}_4\text{Me}\}\{\mu_3\text{-}\eta^2\text{-C}(\text{O})\text{C}(\text{C}_6\text{H}_4\text{Me})=\text{CH}\}]$  **7a** and  $[\text{Os}_3(\text{CO})_7\{\mu\text{-}\eta^2,\eta^3\text{-MeC}_6\text{H}_4\text{CH}=\text{CHC}(\text{C}_6\text{H}_4\text{Me})\text{CH}=\text{CH}\}\{\mu_3\text{-}\eta^2\text{-C}(\text{O})\text{C}(\text{C}_6\text{H}_4\text{Me})=\text{CH}\}]$  **7b** in which the initial displacement of the 2-vinylpyridine is followed by the coupling of two or three *p*-tolylacetylene molecules to the intermediate species. Compounds **6a**, **6b**, **7a** and **7b** have been fully characterised spectroscopically with the crystal structure established for **6b**. Surprisingly, no such reactions occur for the corresponding 4-vinylpyridine derivative.<sup>31</sup>

The molecular structure of complex **6b** is depicted in Fig. 7, together with the atomic numbering scheme. The selected interatomic distances and angles are shown in Table 7. The overall structure is similar to that of **2b** except that two methyl groups on the phenyl rings are observed. The  $^1\text{H}$  NMR spectrum of **6b** shows two equally intense methyl singlets, one at  $\delta$  2.27 and another at  $\delta$  2.35. These results preclude the existence of a pyridine ring in **2b** and hence the rest of the new compounds. The positive FAB mass spectrum of **6b** shows a molecular ion at 1074 which is also consistent with the solid-state structure.

The scope for the alkyne ligand to exhibit different bonding modes increases as the coupling of two or more alkynes to form polymerised alkynes occurs.<sup>32</sup> This is well illustrated by the wide variety of co-ordination modes shown by the hydrocarbyl fragments in compounds **2a**, **2b**, **3a**, **3b**, **5** and **6b** (Table 8). These ligands can donate up to 10 electrons to the cluster unit in **3a** and **3b**. This wide variety of bonding capacity of alkyne-derived ligands to metal clusters naturally arouses great interest in exploring their capabilities as homogeneous catalysts for new reactions or low-energy alternative routes for known organic transformations.<sup>33</sup>

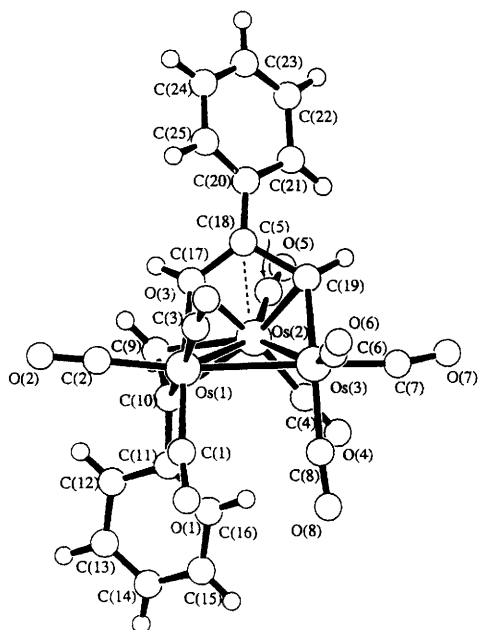


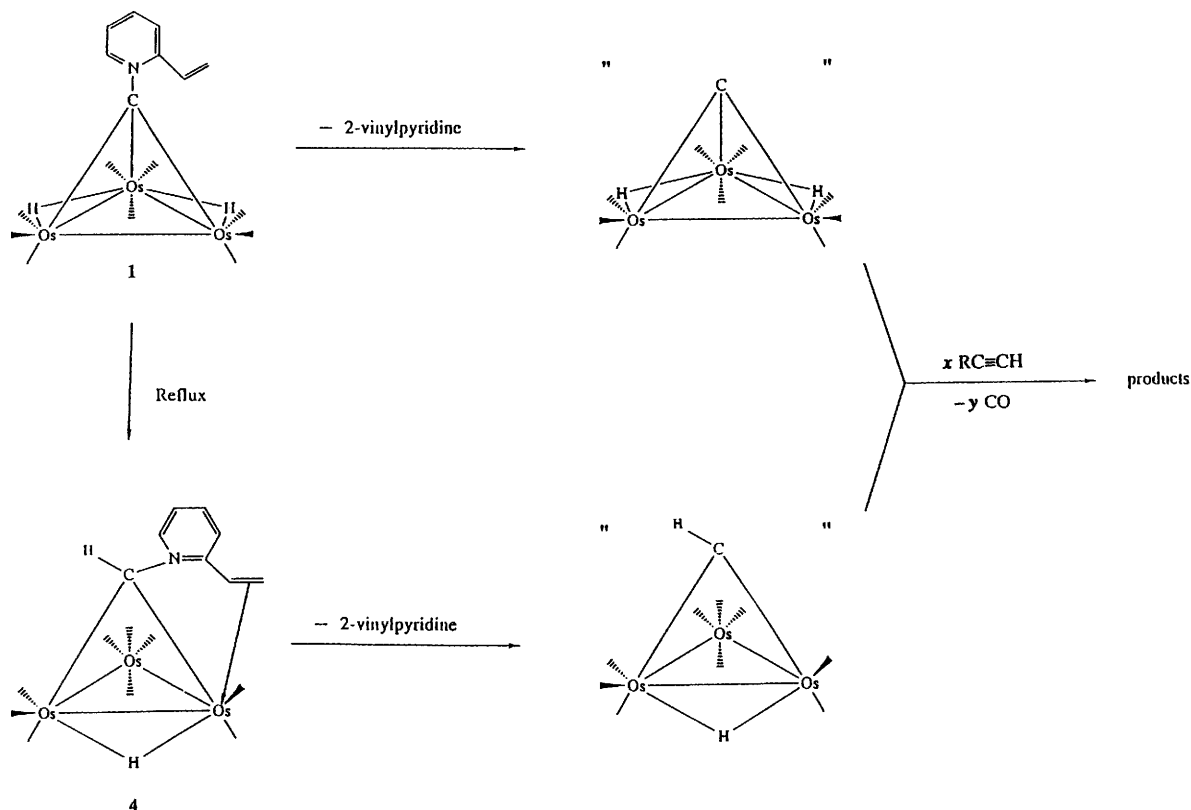
Fig. 6 Molecular structure of complex **5**, showing the atomic labelling scheme

Table 6 Selected bond distances (Å) and angles (°) for complex **5**

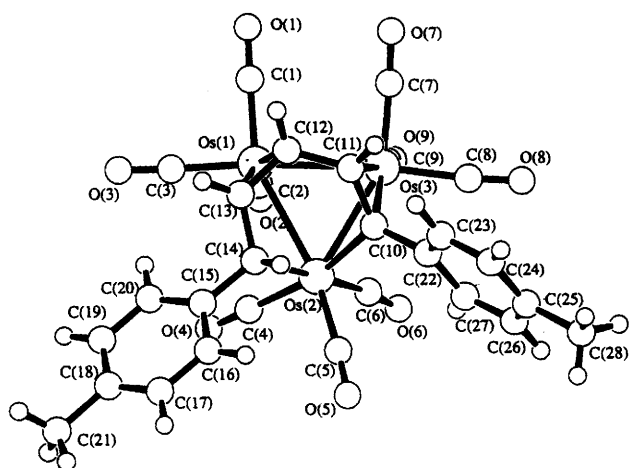
$\text{Os}(1)\text{--}\text{Os}(2)$	2.744(2)	$\text{Os}(2)\text{--}\text{Os}(3)$	2.757(2)
$\text{Os}(1)\text{--}\text{Os}(3)$	2.910(1)	$\text{Os}(1)\text{--}\text{C}(10)$	2.17(4)
$\text{Os}(1)\text{--}\text{C}(17)$	2.18(3)	$\text{Os}(2)\text{--}\text{C}(9)$	2.37(5)
$\text{Os}(2)\text{--}\text{C}(10)$	2.31(4)	$\text{Os}(2)\text{--}\text{C}(17)$	2.15(4)
$\text{Os}(2)\text{--}\text{C}(18)$	2.44(3)	$\text{Os}(2)\text{--}\text{C}(19)$	2.32(4)
$\text{Os}(3)\text{--}\text{C}(19)$	2.06(4)	$\text{C}(9)\text{--}\text{C}(10)$	1.49(6)
$\text{C}(10)\text{--}\text{C}(11)$	1.53(5)	$\text{C}(17)\text{--}\text{C}(18)$	1.46(5)
$\text{C}(18)\text{--}\text{C}(19)$	1.63(6)	$\text{C}(18)\text{--}\text{C}(20)$	1.44(5)
$\text{Os}(2)\text{--}\text{Os}(1)\text{--}\text{Os}(3)$	58.29(5)	$\text{Os}(1)\text{--}\text{Os}(2)\text{--}\text{Os}(3)$	63.86(5)
$\text{Os}(1)\text{--}\text{Os}(3)\text{--}\text{Os}(2)$	57.85(6)	$\text{Os}(1)\text{--}\text{Os}(2)\text{--}\text{C}(9)$	75(1)
$\text{Os}(1)\text{--}\text{Os}(2)\text{--}\text{C}(10)$	49.9(10)	$\text{Os}(1)\text{--}\text{Os}(2)\text{--}\text{C}(17)$	51.3(9)
$\text{Os}(1)\text{--}\text{Os}(2)\text{--}\text{C}(19)$	85(1)	$\text{Os}(2)\text{--}\text{Os}(1)\text{--}\text{C}(17)$	50(1)
$\text{Os}(2)\text{--}\text{Os}(3)\text{--}\text{C}(19)$	55(1)	$\text{Os}(3)\text{--}\text{Os}(2)\text{--}\text{C}(9)$	138(1)
$\text{Os}(3)\text{--}\text{Os}(2)\text{--}\text{C}(10)$	103.8(10)	$\text{Os}(3)\text{--}\text{Os}(2)\text{--}\text{C}(17)$	89.6(9)
$\text{Os}(3)\text{--}\text{Os}(2)\text{--}\text{C}(19)$	46(1)	$\text{Os}(1)\text{--}\text{C}(10)\text{--}\text{C}(9)$	118(3)
$\text{Os}(1)\text{--}\text{C}(17)\text{--}\text{C}(18)$	122(2)	$\text{Os}(3)\text{--}\text{C}(19)\text{--}\text{C}(18)$	124(2)
$\text{C}(17)\text{--}\text{Os}(2)\text{--}\text{C}(19)$	71(1)	$\text{C}(17)\text{--}\text{C}(18)\text{--}\text{C}(19)$	114(3)

Table 7 Selected bond distances (Å) and angles (°) for complex **6b**

$\text{Os}(1)\text{--}\text{Os}(2)$	2.844(1)	$\text{Os}(2)\text{--}\text{Os}(3)$	2.855(1)
$\text{Os}(1)\text{--}\text{Os}(3)$	2.811(1)	$\text{Os}(1)\text{--}\text{C}(12)$	2.31(1)
$\text{Os}(1)\text{--}\text{C}(13)$	2.36(1)	$\text{Os}(2)\text{--}\text{C}(10)$	2.16(1)
$\text{Os}(2)\text{--}\text{C}(14)$	2.28(1)	$\text{Os}(3)\text{--}\text{C}(10)$	2.220(10)
$\text{Os}(3)\text{--}\text{C}(11)$	2.31(1)	$\text{Os}(2)\text{--}\text{C}(11)$	1.41(1)
$\text{C}(10)\text{--}\text{C}(22)$	1.50(1)	$\text{C}(11)\text{--}\text{C}(12)$	1.46(1)
$\text{C}(12)\text{--}\text{C}(13)$	1.41(1)	$\text{C}(13)\text{--}\text{C}(14)$	1.48(1)
$\text{C}(14)\text{--}\text{C}(15)$	1.51(1)		
$\text{Os}(2)\text{--}\text{Os}(1)\text{--}\text{Os}(3)$	60.64(2)	$\text{Os}(1)\text{--}\text{Os}(2)\text{--}\text{Os}(3)$	59.10(2)
$\text{Os}(1)\text{--}\text{Os}(3)\text{--}\text{Os}(2)$	60.26(2)	$\text{Os}(1)\text{--}\text{Os}(2)\text{--}\text{C}(10)$	87.3(3)
$\text{Os}(1)\text{--}\text{Os}(2)\text{--}\text{C}(14)$	75.5(3)	$\text{Os}(2)\text{--}\text{Os}(1)\text{--}\text{C}(12)$	77.8(3)
$\text{Os}(2)\text{--}\text{Os}(1)\text{--}\text{C}(13)$	68.6(3)	$\text{Os}(2)\text{--}\text{Os}(3)\text{--}\text{C}(10)$	48.4(3)
$\text{Os}(2)\text{--}\text{Os}(3)\text{--}\text{C}(11)$	70.7(3)	$\text{Os}(3)\text{--}\text{Os}(2)\text{--}\text{C}(10)$	50.2(3)
$\text{Os}(3)\text{--}\text{Os}(2)\text{--}\text{C}(14)$	108.4(3)	$\text{Os}(1)\text{--}\text{C}(12)\text{--}\text{C}(11)$	107.8(7)
$\text{Os}(1)\text{--}\text{C}(13)\text{--}\text{C}(14)$	109.1(7)	$\text{Os}(2)\text{--}\text{C}(10)\text{--}\text{C}(11)$	113.9(7)
$\text{Os}(2)\text{--}\text{C}(14)\text{--}\text{C}(13)$	101.8(7)	$\text{C}(10)\text{--}\text{Os}(2)\text{--}\text{C}(14)$	77.9(4)
$\text{C}(10)\text{--}\text{C}(11)\text{--}\text{C}(12)$	125.2(10)	$\text{C}(11)\text{--}\text{C}(10)\text{--}\text{C}(22)$	121.0(9)
$\text{C}(11)\text{--}\text{C}(12)\text{--}\text{C}(13)$	120(1)	$\text{C}(12)\text{--}\text{C}(13)\text{--}\text{C}(14)$	121(1)
$\text{C}(13)\text{--}\text{C}(14)\text{--}\text{C}(15)$	117.2(10)		



Scheme 2

Fig. 7 Molecular structure of complex **6b**, showing the atomic labelling scheme**Table 8** Modes of co-ordination exhibited by the various hydrocarbyl fragments in compounds **2a**, **2b**, **3a**, **3b**, **5** and **6b** and the total number of electrons they contribute

Compound	Co-ordination modes	No. of electrons contributed
<b>2a</b>	$\mu_3\text{-}\eta^3$	5
<b>2b</b>	$\mu_3\text{-}\eta^1, \eta^2, \eta^2, \eta^1$	6
<b>3a</b>	$\mu\text{-}\eta^2, \eta^3$ and $\mu_3\text{-}\eta^2$	10
<b>3b</b>	$\mu\text{-}\eta^2, \eta^3$ and $\mu_3\text{-}\eta^2$	10
<b>5</b>	$\mu_3\text{-}\eta^3$ and $\mu\text{-}\eta^2$	8
<b>6b</b>	$\mu_3\text{-}\eta^1, \eta^2, \eta^2, \eta^1$	6

### Conclusion

The alkyldiene cluster **1** provides a viable high-yield route to alkyne-containing clusters by a new alkyldiene-alkyne coupling

reaction sequence. Such facile addition of unsaturated hydrocarbyl ligands into the proposed intermediates represents a potentially powerful system for investigating the chemistry of this class of compounds. Mechanistic information regarding carbon-carbon bond formation on the surface of a cluster can also be obtained. A variety of interesting studies suggest that surface carbon and/or CH, CH<sub>2</sub> and CH<sub>3</sub> radicals on the surface may be intermediates in the Fischer-Tropsch synthesis.<sup>34,35</sup> For instance, surface carbon on an alumina-supported Ni catalyst (Ni<sub>3</sub>C) can be conveniently prepared and its subsequent hydrogenation at high temperature is rapid enough to be a possible intermediate in methanation.<sup>36</sup> Extensive studies have also been carried out on tetranuclear carbido clusters of iron<sup>37</sup> and ruthenium.<sup>38</sup> It is believed that the formation of a  $\mu_3$ -carbide [Os<sub>3</sub>( $\mu\text{-H}$ )<sub>2</sub>(CO)<sub>9</sub>( $\mu_3\text{-C}$ )] or a  $\mu$ -alkylidene CH fragment [Os<sub>3</sub>( $\mu\text{-H}$ )(CO)<sub>9</sub>( $\mu\text{-CH}$ )] occurs upon reaction although the isolation of these reactive species is elusive. These intermediate species possibly represent a particularly attractive analogue of a  $\mu_3$ -carbide or  $\mu$ -alkylidene CH fragment observed on a trimetallic surface and are convenient models for examining their roles in the Fischer-Tropsch reaction mechanism.

Regardless of the importance of this alkyldiene cluster chemistry to surface chemistry, the formation of various novel hydrocarbyl fragments on a metal surface is intrinsically interesting. Hydrogenation of the alkynes has been shown to take place through such cluster-assisted reactions. Usually, the reactions are accompanied by skeletal rearrangements and hydrogen transfers. Such rearrangement on metal clusters is noteworthy because it could allow the hydrocarbyl fragments to be considered as possible intermediates of catalytic alkyne metathesis.

### Experimental

None of the compounds reported is particularly air-sensitive, however, all reactions were carried out under an atmosphere of dry dinitrogen using standard Schlenk techniques and



Table 9 Crystal data and data collection parameters for 2a, 2b, 3a, 3b, 5 and 6b

Compound	2a	2b	3a	3b	5	6b
Formula	Os <sub>3</sub> C <sub>26</sub> H <sub>14</sub> O <sub>9</sub>	Os <sub>3</sub> C <sub>26</sub> H <sub>14</sub> O <sub>9</sub>	Os <sub>3</sub> C <sub>33</sub> H <sub>20</sub> O <sub>8</sub>	Os <sub>3</sub> C <sub>33</sub> H <sub>20</sub> O <sub>8</sub>	Os <sub>3</sub> C <sub>25</sub> H <sub>14</sub> O <sub>8</sub>	Os <sub>3</sub> C <sub>28</sub> H <sub>19</sub> O <sub>9</sub>
<i>M</i>	1040.86	1040.86	1114.93	1114.93	1012.85	1068.88
Colour, habit	Yellow, rods	Orange, blocks	Red, blocks	Red, plates	Red, needles	Red, rods
Crystal size/mm	0.18 × 0.20 × 0.32	0.16 × 0.18 × 0.26	0.19 × 0.29 × 0.32	0.06 × 0.14 × 0.22	0.10 × 0.11 × 0.34	0.18 × 0.20 × 0.30
Crystal system	Monoclinic	Monoclinic	Monoclinic	Triclinic	Orthorhombic	Triclinic
Space group	<i>P</i> 2 <sub>1</sub> / <i>n</i> (no. 14)	<i>P</i> 2 <sub>1</sub> / <i>c</i> (no. 14)	<i>P</i> 2 <sub>1</sub> / <i>c</i> (no. 14)	<i>P</i> 1̄ (no. 2)	<i>Fdd</i> 2 (no. 43)	<i>P</i> 1̄ (no. 2)
<i>a</i> /Å	9.648(4)	8.765(4)	8.711(4)	10.514(4)	31.170(7)	9.659(2)
<i>b</i> /Å	11.769(2)	9.399(4)	30.792(6)	15.948(5)	37.850(4)	17.674(3)
<i>c</i> /Å	24.484(10)	31.836(13)	12.004(4)	9.684(5)	8.753(3)	8.863(2)
<i>a</i> /°	90.0	90.0	90.0	100.72(4)	90.0	99.83(2)
<i>β</i> /°	96.17(3)	97.66(4)	101.45(3)	103.67(4)	90.0	92.91(2)
<i>γ</i> /°	90.0	90.0	90.0	102.11(3)	90.0	105.09(1)
<i>U</i> /Å <sup>3</sup>	2764(2)	2599(3)	3155(1)	1494(1)	10326(3)	1432.2(5)
<i>Z</i>	4	4	4	2	16	2
<i>D</i> <sub>c</sub> /g cm <sup>-3</sup>	2.501	2.660	2.347	2.478	2.606	2.479
<i>F</i> (000)	1880	1880	2040	1020	7296	972
<i>μ</i> (Mo-Kα)/cm <sup>-1</sup>	138.05	147.04	120.91	127.65	147.65	133.18
<i>T</i> /K	296.0	296.0	296.0	298.0	298.0	298.0
Diffractometer	Enraf-Nonius CAD4	Enraf-Nonius CAD4	Rigaku AFC7R	Rigaku AFC7R	Rigaku AFC7R	Rigaku AFC7R
2θ range/°	2.0–45.0	2.0–45.0	4.0–45.0	4.0–45.0	4.0–45.0	4.0–45.0
Scan speed (in ω)/° min <sup>-1</sup>	8.4	16.8	16.0	16.0	16.0	16.0
Scan width/°	0.65 + 0.34 tan θ	0.55 + 0.34 tan θ	0.79 + 0.35 tan θ	0.73 + 0.35 tan θ	1.21 + 0.35 tan θ	1.10 + 0.35 tan θ
Transmission factors	0.7526–1.0	0.4199–1.0	0.7349–1.0	0.3930–1.0	0.9339–1.0	0.6369–1.0
Reflections collected	4101	3924	4558	4164	1900	4022
Unique reflections	3567	3362	4240	3906	1900	3752
Observed reflections [ <i>I</i> > 3σ( <i>I</i> )]	2606	2484	1943	2469	1456	3138
<i>R</i>	0.037	0.062	0.045	0.059	0.047	0.029
<i>R</i> '	0.041	0.077	0.049	0.078	0.054	0.030
<i>g</i> in weighting scheme	0.04	0.04	0.022	0.002	0.007	0.003
Max. residuals/e Å <sup>-3</sup>	1.341 (close to Os)	2.715 (close to Os)	0.88	2.10 (close to Os)	2.21 (close to Os)	1.10 (close to Os)

Details in common: scan type ω–2θ; absorption correction, ψ scan; weighting scheme  $w = [\sigma^2(F_o^2) + g(F_o^2)]^{-1}$ .

monitored by solution IR spectroscopy (CO stretching region). Dichloromethane was dried over  $\text{CaH}_2$  and *n*-hexane was distilled from sodium-benzophenone. Acetone (AR grade) was dried over 4 Å molecular sieves. The starting cluster **1** was prepared as described previously.<sup>6</sup> All other reagents were purchased from Aldrich and used as received. Infrared spectra were recorded on a Bio-Rad FTS-7 IR spectrometer using 0.5 mm solution cells. The  $^1\text{H}$  NMR and  $^1\text{H}$ - $^1\text{H}$  COSY spectra were recorded on a JEOL GSX 270 FT-NMR spectrometer [ $\text{SiMe}_4$  reference ( $\delta$  0)]. Mass spectra were recorded on a Finnigan MAT 95 instrument with the fast atom bombardment (FAB) technique. Routine separation of products was performed in the air by thin-layer chromatography with plates coated with Merck Kieselgel 60 GF<sub>254</sub>.

**Thermal Reaction of  $[\text{Os}_3(\mu\text{-H})_2(\text{CO})_9(\mu_3\text{-CNC}_5\text{H}_4\text{CH}=\text{CH}_2)]$  **1** with Phenylacetylene.**—To a solution of **1** (60 mg, 0.064 mmol) in *n*-hexane (100 cm<sup>3</sup>) was added an excess of phenylacetylene (33 mg, 0.32 mmol). The reaction mixture was heated to reflux at 60 °C for 6 h during which time the reaction solution changed from deep purple to orange-brown. Excess solvent was then removed under reduced pressure, yielding a brown oily residue. This residue was dissolved in the minimum amount of dichloromethane and subjected to preparative TLC on silica using *n*-hexane-acetone (95:5 v/v) as eluent to afford four bands. The first yellow band eluted was identified as **2a** (20 mg, 0.019 mmol, 30%), the second orange fraction as **2b** (16 mg, 0.015 mmol, 24%) and the third yellow band as **4** (4 mg, 0.004 mmol, 7%). The remaining red fraction was subjected to TLC again using dichloromethane as eluent. Complex **3b** was isolated as a red-orange product (4 mg, 0.004 mmol, 6%) from the first band while the isomeric compound **3a** was collected as a red product from the second band (6 mg, 0.005 mmol, 8%). (Found for **2a**: C, 30.15; H, 1.20. Calc. for  $\text{C}_{26}\text{H}_{14}\text{O}_9\text{Os}_3$ : C, 30.00; H, 1.35%. Found for **2b**: C, 30.50; H, 1.40. Calc. for  $\text{C}_{26}\text{H}_{14}\text{O}_9\text{Os}_3$ : C, 30.00; H, 1.35%).

**Reaction of **1** with Phenylacetylene in Acetone at Ambient Temperature.**—An acetone solution of complex **1** (60 mg in 50 cm<sup>3</sup>, 0.064 mmol) was allowed to stir at room temperature in the presence of a large excess of phenylacetylene (33 mg, 0.32 mmol). After 8 h, the mixture turned from red-orange to yellow-orange. Both TLC and IR spectroscopy showed that all the starting material had been consumed. Excess solvent was removed under reduced pressure to leave a brown-orange residue. The residue was extracted into dichloromethane and purified by chromatography on silica gel plates. Elution with *n*-

hexane- $\text{CH}_2\text{Cl}_2$  (80:20, v/v) afforded a major orange product identified as **5** (22 mg, 0.022 mmol, 34%) (Found: C, 29.50; H, 1.25. Calc. for  $\text{C}_{25}\text{H}_{14}\text{O}_8\text{Os}_3$ : C, 29.65; H, 1.30%).

**Thermal Reaction of **1** with *p*-Tolylacetylene.**—The same procedures apply as above except that *p*-tolylacetylene (37 mg, 0.32 mmol) was used instead of phenylacetylene. Preparative TLC led to the isolation of five compounds, identified as  $[\text{Os}_3(\mu\text{-H})(\text{CO})_9\{\mu\text{-C}(\text{H})\text{NC}_5\text{H}_4(\eta^2\text{-CH}=\text{CH}_2)\}]$  **4** (4 mg, 0.004 mmol, 7%),  $[\text{Os}_3(\mu\text{-H})(\text{CO})_9\{\mu_3\text{-}\eta^3\text{-MeC}_6\text{H}_4\text{CCHCCH}=\text{CH}(\text{C}_6\text{H}_4\text{Me})\}]$  **6a** (20 mg, 0.019 mmol, 29%),  $[\text{Os}_3(\text{CO})_9(\mu_3\text{-}\eta^1, \eta^2, \eta^2, \eta^1\text{-MeC}_6\text{H}_4\text{CHCH}=\text{CHCH}=\text{CC}_6\text{H}_4\text{Me})]$  **6b** (17 mg, 0.016 mmol, 25%),  $[\text{Os}_3(\text{CO})_7\{\mu\text{-}\eta^2, \eta^3\text{-CH}_2=\text{CHC}(\text{C}_6\text{H}_4\text{Me})\text{-CHCC}_6\text{H}_4\text{Me}\}\{\mu_3\text{-}\eta^2\text{-C}(\text{O})\text{C}(\text{C}_6\text{H}_4\text{Me})=\text{CH}\}]$  **7a** (6 mg, 0.005 mmol, 8%) and  $[\text{Os}_3(\text{CO})_7\{\mu\text{-}\eta^2, \eta^3\text{-MeC}_6\text{H}_4\text{CH}=\text{CHC}(\text{C}_6\text{H}_4\text{Me})\text{CHCH}\}\{\mu_3\text{-}\eta^2\text{-C}(\text{O})\text{C}(\text{C}_6\text{H}_4\text{Me})=\text{CH}\}]$  **7b** (5 mg, 0.004 mmol, 7%).

**X-Ray Data Collection, Solution and Refinement.**—Bright yellow crystals of complex **2a** suitable for diffraction study were grown from a saturated solution of **2a** in *n*-hexane at -10 °C for a period of 5 d. Orange crystals of **2b** and **5** were grown by slow evaporation of their respective *n*-hexane solutions at -5 °C for 2 d. Red crystals of **3a**, **3b** and **6b** were grown by slow evaporation of their respective *n*-hexane- $\text{CH}_2\text{Cl}_2$  solutions at room temperature for 2 d. Crystals suitable for X-ray diffraction were glued on glass fibres with epoxy resin and mounted on an Enraf-Nonius CAD4 (**2a** and **2b**) or Rigaku AFC7R diffractometer (**3a**, **3b**, **5** and **6b**) using graphite-monochromated Mo- $\text{K}\alpha$  radiation ( $\lambda = 0.71069$  Å) for unit-cell determination and data collection. Details of the intensity data collection are given in Table 9. The osmium atoms were found by direct methods (MULTAN for **2a** and **2b**;<sup>39</sup> SAPI91 for **3a**;<sup>40</sup> SIR88 for **6b**<sup>41</sup>) or Patterson methods (**3b** and **5**). The molecular structures were obtained by subsequent Fourier and Fourier-difference syntheses. The intensity data were corrected for Lorentz-polarisation effects and semi-empirical absorption corrections ( $\psi$ -scan method) were also applied.<sup>42</sup> Atomic coordinates and thermal parameters were refined by full-matrix least-squares analysis, with the osmium atoms refined anisotropically. The hydrogen atoms of the organic moieties were generated in their ideal positions (C-H, 0.95 Å) while the metal hydride in **2a** was estimated by potential energy calculations.<sup>15</sup> Calculations were performed either on a MicroVAX (**2a** and **2b**) or a Silicon-Graphics (**3a**, **3b**, **5** and **6**) computer using the program packages SDP<sup>43</sup> or TEXSAN.<sup>44</sup> Final atomic coordinates for **2a**, **2b**, **3a**, **3b**, **5** and **6b** are listed in Tables 10–15 respectively.

**Table 10** Atomic coordinates for  $[\text{Os}_3(\mu\text{-H})(\text{CO})_9\{\mu_3\text{-}\eta^3\text{-PhCCHC}(\text{CH}=\text{CHPh})\}]$  **2a**

Atom	x	y	z	Atom	x	y	z
Os(1)	0.610 73(6)	0.176 19(5)	0.159 57(3)	C(17)	0.102(2)	-0.051(2)	0.072 2(7)
Os(2)	0.358 67(6)	0.202 93(6)	0.206 06(2)	C(18)	0.173(2)	-0.120(2)	0.036 5(8)
Os(3)	0.538 12(6)	0.399 41(5)	0.187 71(3)	C(19)	0.315(2)	-0.094(2)	0.030 9(9)
C(1)	0.768(2)	0.178(2)	0.122 3(7)	C(20)	0.381(2)	0.002(2)	0.058 8(7)
C(2)	0.709(2)	0.191(1)	0.228 8(7)	C(21)	0.735(2)	0.537(2)	0.018 6(8)
C(3)	0.607(2)	0.018(2)	0.162 2(8)	C(22)	0.764(2)	0.474(2)	-0.025 0(8)
C(4)	0.171(2)	0.236(1)	0.209 2(6)	C(23)	0.855(3)	0.522(2)	-0.066(1)
C(5)	0.333(2)	0.051(2)	0.217 8(7)	C(24)	0.890(2)	0.631(2)	-0.057 9(9)
C(6)	0.404(2)	0.222(2)	0.283 8(7)	C(25)	0.860(2)	0.694(2)	-0.019 8(9)
C(7)	0.459(2)	0.539(2)	0.170 7(7)	C(26)	0.777(2)	0.654(2)	0.024 8(9)
C(8)	0.724(2)	0.447(1)	0.185 0(6)	O(1)	0.867(1)	0.181(1)	0.097 9(5)
C(9)	0.552(2)	0.435(2)	0.263 6(7)	O(2)	0.769(1)	0.200(1)	0.272 3(5)
C(10)	0.654(2)	0.490(2)	0.063 0(7)	O(3)	0.610(2)	-0.082(1)	0.165 2(6)
C(11)	0.608(2)	0.383(1)	0.063 7(6)	O(4)	0.049(1)	0.254(1)	0.205 9(5)
C(12)	0.532(1)	0.334(1)	0.108 5(6)	O(5)	0.316(1)	-0.047(1)	0.226 0(6)
C(13)	0.453(1)	0.235(1)	0.089 6(6)	O(6)	0.434(1)	0.238(1)	0.330 8(6)
C(14)	0.376(1)	0.166(1)	0.123 4(6)	O(7)	0.406(1)	0.627(1)	0.158 3(6)
C(15)	0.308(1)	0.067(1)	0.093 6(5)	O(8)	0.841(1)	0.473(1)	0.186 4(5)
C(16)	0.169(2)	0.040(1)	0.100 6(7)	O(9)	0.563(1)	0.457(1)	0.310 3(5)

**Table 11** Atomic coordinates for  $[\text{Os}_3(\text{CO})_9(\mu_3\text{-}\eta^1, \eta^2, \eta^2, \eta^1\text{-PhCHCH=CHCH=CPh})] \mathbf{2b}$ 

Atom	x	y	z	Atom	x	y	z
Os(1)	0.646 6(1)	-0.947 1(1)	0.100 41(3)	C(17)	0.074(3)	-0.604(3)	0.228 2(9)
Os(2)	0.399 4(1)	-0.758 24(9)	0.110 63(3)	C(18)	0.048(3)	-0.457(3)	0.220 2(8)
Os(3)	0.461 3(1)	-0.999 5(1)	0.164 17(3)	C(19)	0.147(3)	-0.384(3)	0.198 5(8)
C(1)	0.808(3)	-1.057(3)	0.124 2(9)	C(20)	0.279(3)	-0.451(2)	0.185 6(8)
C(2)	0.545(4)	-1.095(3)	0.067(1)	C(21)	0.724(3)	-0.608(2)	0.095 8(7)
C(3)	0.763(3)	-0.895(3)	0.055 5(9)	C(22)	0.848(3)	-0.534(3)	0.117 6(8)
C(4)	0.370(3)	-0.564(2)	0.092 2(8)	C(23)	0.922(3)	-0.429(3)	0.093 1(9)
C(5)	0.192(3)	-0.796(3)	0.119 8(8)	C(24)	0.881(4)	-0.414(3)	0.052(1)
C(6)	0.359(3)	-0.834(3)	0.055 7(9)	C(25)	0.748(4)	-0.481(3)	0.030(1)
C(7)	0.589(3)	-1.158(3)	0.182 6(8)	C(26)	0.675(3)	-0.585(3)	0.052 1(9)
C(8)	0.323(3)	-1.096(3)	0.124 0(8)	O(1)	0.913(2)	-1.115(2)	0.143 6(7)
C(9)	0.336(3)	-1.021(3)	0.206 4(9)	O(2)	0.488(2)	-1.191(2)	0.047 3(7)
C(10)	0.646(3)	-0.723(2)	0.119 0(7)	O(3)	0.833(3)	-0.872(2)	0.028 5(7)
C(11)	0.727(3)	-0.788(2)	0.155 2(8)	O(4)	0.345(2)	-0.451(2)	0.081 9(7)
C(12)	0.647(3)	-0.844(3)	0.190 8(8)	O(5)	0.070(2)	-0.821(2)	0.125 6(7)
C(13)	0.514(3)	-0.780(2)	0.202 3(8)	O(6)	0.317(2)	-0.870(2)	0.022 4(7)
C(14)	0.444(3)	-0.663(2)	0.177 5(8)	O(7)	0.654(2)	-1.262(2)	0.189 7(7)
C(15)	0.305(3)	-0.597(2)	0.193 4(8)	O(8)	0.225(3)	-1.154(2)	0.102 8(7)
C(16)	0.198(3)	-0.674(3)	0.213 5(9)	O(9)	0.272(3)	-1.040(2)	0.236 8(7)

**Table 12** Atomic coordinates for  $[\text{Os}_3(\text{CO})_7\{\mu\text{-}\eta^2, \eta^3\text{-CH}_2\text{=CHC(Ph)CHCPh}\}\{\mu_3\text{-}\eta^2\text{-C(O)C(Ph)=CH}\}] \mathbf{3a}$ 

Atom	x	y	z	Atom	x	y	z
Os(1)	-0.054 5(1)	0.157 82(4)	0.287 09(10)	C(12)	0.428(4)	0.056(1)	0.526(3)
Os(2)	0.134 5(1)	0.118 83(4)	0.157 39(10)	C(13)	0.497(4)	0.036(1)	0.628(3)
Os(3)	-0.014 9(1)	0.065 71(4)	0.285 21(10)	C(14)	0.428(4)	0.035(1)	0.724(3)
O(1)	-0.056(3)	0.240 3(8)	0.424(2)	C(15)	0.288(4)	0.051(1)	0.714(3)
O(2)	-0.351(3)	0.124 8(7)	0.364(2)	C(16)	0.206(3)	0.069 4(9)	0.610(2)
O(3)	0.460(3)	0.127 3(8)	0.110(2)	C(17)	-0.229(3)	0.196 4(9)	0.148(2)
O(4)	0.081(2)	0.046 6(7)	-0.015(2)	C(18)	-0.186(3)	0.159 6(9)	0.104(2)
O(5)	-0.300(3)	0.049 8(7)	0.097(2)	C(19)	-0.056(3)	0.158 3(8)	0.036(2)
O(6)	0.108(2)	-0.024 1(7)	0.255(2)	C(20)	0.077(3)	0.183 9(8)	0.084(2)
O(7)	-0.169(2)	0.037 5(7)	0.482(2)	C(21)	0.115(3)	0.187 5(8)	0.204(2)
O(8)	0.136(2)	0.156 2(7)	0.521(2)	C(22)	-0.099(3)	0.148 7(9)	-0.087(2)
C(1)	-0.059(4)	0.208(1)	0.371(3)	C(23)	-0.250(4)	0.136 9(10)	-0.139(3)
C(2)	-0.231(4)	0.137 6(9)	0.342(3)	C(24)	-0.293(5)	0.131(1)	-0.260(4)
C(3)	0.336(4)	0.123 9(10)	0.134(3)	C(25)	-0.183(6)	0.140(1)	-0.311(4)
C(4)	0.105(3)	0.073 2(10)	0.055(3)	C(26)	-0.044(6)	0.152(2)	-0.275(4)
C(5)	-0.193(3)	0.054 8(10)	0.173(3)	C(27)	0.013(5)	0.157(1)	-0.156(4)
C(6)	0.062(3)	0.010 8(9)	0.268(2)	C(28)	0.244(3)	0.215 1(9)	0.259(2)
C(7)	-0.111(3)	0.048 7(9)	0.406(2)	C(29)	0.255(4)	0.256(1)	0.205(3)
C(8)	0.115(3)	0.136 5(9)	0.432(2)	C(30)	0.372(6)	0.282(2)	0.244(4)
C(9)	0.233(3)	0.087 4(8)	0.307(2)	C(31)	0.474(6)	0.274(2)	0.340(4)
C(10)	0.199(3)	0.096 4(9)	0.410(3)	C(32)	0.482(5)	0.237(1)	0.402(4)
C(11)	0.277(3)	0.072 7(8)	0.518(2)	C(33)	0.356(4)	0.205(1)	0.349(3)

**Table 13** Atomic coordinates for  $[\text{Os}_3(\text{CO})_7\{\mu\text{-}\eta^2, \eta^3\text{-PhCH=CHC(Ph)CHCH}\}\{\mu_3\text{-}\eta^2\text{-C(O)C(Ph)=CH}\}] \mathbf{3b}$ 

Atom	x	y	z	Atom	x	y	z
Os(1)	0.331 9(1)	0.287 94(9)	-0.102 5(2)	C(12)	0.037(4)	0.331(3)	0.292(5)
Os(2)	0.231 9(1)	0.136 01(9)	-0.024 4(2)	C(13)	-0.052(5)	0.369(3)	0.357(5)
Os(3)	0.045 7(1)	0.211 10(9)	-0.164 8(2)	C(14)	-0.122(4)	0.425(3)	0.293(5)
O(1)	0.576(3)	0.442(2)	0.078(3)	C(15)	-0.109(4)	0.441(2)	0.167(4)
O(2)	0.234(3)	0.386(2)	-0.333(3)	C(16)	-0.029(4)	0.400(2)	0.087(4)
O(3)	0.018(3)	-0.035(2)	-0.185(3)	C(17)	0.430(3)	0.221(2)	0.033(3)
O(4)	0.292(3)	0.075(2)	0.258(3)	C(18)	0.431(4)	0.135(2)	-0.044(4)
O(5)	-0.226(3)	0.126(2)	-0.134(3)	C(19)	0.357(4)	0.106(3)	-0.179(4)
O(6)	-0.063(3)	0.349(2)	-0.290(3)	C(20)	0.345(4)	0.170(3)	-0.269(4)
O(7)	0.008(3)	0.099(2)	-0.469(3)	C(21)	0.467(3)	0.239(2)	-0.246(4)
O(8)	0.276(3)	0.435(2)	0.091(3)	C(22)	0.494(3)	0.296(2)	-0.357(4)
C(1)	0.479(3)	0.383(2)	-0.006(4)	C(23)	0.403(3)	0.279(2)	-0.502(4)
C(2)	0.258(4)	0.344(2)	-0.252(4)	C(24)	0.430(4)	0.330(2)	-0.590(4)
C(3)	0.097(3)	0.031(2)	-0.121(4)	C(25)	0.544(4)	0.400(3)	-0.547(5)
C(4)	0.269(4)	0.098(2)	0.147(4)	C(26)	0.632(5)	0.413(3)	-0.415(5)
C(5)	-0.117(4)	0.158(3)	-0.148(5)	C(27)	0.603(4)	0.365(2)	-0.319(4)
C(6)	-0.016(4)	0.295(3)	-0.249(5)	C(28)	0.338(3)	0.010(2)	-0.269(4)
C(7)	0.026(3)	0.142(2)	-0.343(4)	C(29)	0.315(4)	-0.061(3)	-0.211(4)
C(8)	0.240(3)	0.353(2)	0.040(3)	C(30)	0.300(4)	-0.152(3)	-0.285(5)
C(9)	0.127(3)	0.208(2)	0.068(3)	C(31)	0.323(4)	-0.163(3)	-0.419(4)
C(10)	0.129(3)	0.300(2)	0.073(3)	C(32)	0.351(4)	-0.098(3)	-0.483(5)
C(11)	0.043(3)	0.340(2)	0.157(4)	C(33)	0.355(4)	-0.008(3)	-0.414(4)

**Table 14** Atomic coordinates for  $[\text{Os}_3(\text{CO})_9(\mu-\eta^2\text{-PhCCH}_2)(\mu_3-\eta^3\text{-CHCPhCH})] \mathbf{5}$ 

Atom	x	y	z	Atom	x	y	z
Os(1)	0.664 67(5)	0.075 74(4)	0.677 8	C(8)	0.638(2)	0.110(2)	0.313(7)
Os(2)	0.645 93(5)	0.019 55(4)	0.491 2(3)	C(9)	0.708(1)	0.001(1)	0.626(5)
Os(3)	0.600 59(5)	0.080 83(4)	0.437 0	C(10)	0.711(1)	0.039(1)	0.583(5)
O(1)	0.708(1)	0.145 4(9)	0.552(4)	C(11)	0.748(1)	0.052 3(8)	0.481(4)
O(2)	0.720(1)	0.072 6(10)	0.976(6)	C(12)	0.788(1)	0.044(1)	0.544(5)
O(3)	0.588(1)	0.113 7(10)	0.833(5)	C(13)	0.823(1)	0.055 6(10)	0.466(5)
O(4)	0.663(1)	0.030 9(8)	0.167(5)	C(14)	0.821(1)	0.073(1)	0.336(5)
O(5)	0.632(1)	-0.057(1)	0.423(5)	C(15)	0.782(1)	0.084(1)	0.277(5)
O(6)	0.541(1)	0.141 6(9)	0.542(4)	C(16)	0.747(1)	0.073(1)	0.353(5)
O(7)	0.544(1)	0.064(1)	0.161(6)	C(17)	0.634(1)	0.025 4(9)	0.732(5)
O(8)	0.660(1)	0.128 0(9)	0.227(5)	C(18)	0.590(1)	0.016 8(9)	0.687(5)
C(1)	0.695(1)	0.119(1)	0.603(5)	C(19)	0.575(1)	0.035(1)	0.527(6)
C(2)	0.696(2)	0.076(1)	0.864(7)	C(20)	0.566(1)	-0.012 7(9)	0.743(5)
C(3)	0.618(2)	0.101(1)	0.779(7)	C(21)	0.547(1)	-0.038(1)	0.647(6)
C(4)	0.659(1)	0.025(1)	0.288(5)	C(22)	0.523(1)	-0.065(1)	0.723(6)
C(5)	0.637(1)	-0.028(1)	0.459(5)	C(23)	0.521(1)	-0.065(1)	0.870(5)
C(6)	0.563(1)	0.119(1)	0.489(6)	C(24)	0.540(2)	-0.043(1)	0.954(7)
C(7)	0.567(2)	0.074(1)	0.258(6)	C(25)	0.561(1)	-0.017(1)	0.891(5)

**Table 15** Atomic coordinates for  $[\text{Os}_3(\text{CO})_9(\mu_3-\eta^1, \eta^2, \eta^2, \eta^1\text{-MeC}_6\text{H}_4\text{CHCH=CHCH=CC}_6\text{H}_4\text{Me})] \mathbf{6b}$ 

Atom	x	y	z	Atom	x	y	z
Os(1)	0.365 50(5)	0.180 76(3)	0.488 27(5)	C(9)	0.562(1)	0.362 7(8)	0.422(2)
Os(2)	0.191 72(5)	0.287 16(3)	0.558 44(5)	C(10)	0.140(1)	0.272 9(6)	0.313(1)
Os(3)	0.378 10(5)	0.302 73(3)	0.318 92(5)	C(11)	0.167(1)	0.204 9(7)	0.227(1)
O(1)	0.559(1)	0.103 6(7)	0.293(1)	C(12)	0.185(1)	0.135 6(7)	0.287(1)
O(2)	0.600(1)	0.295 5(6)	0.723(1)	C(13)	0.119(1)	0.115 4(7)	0.419(1)
O(3)	0.339(1)	0.054 1(7)	0.687(1)	C(14)	0.032(1)	0.163 7(6)	0.501(1)
O(4)	0.255 6(9)	0.262 6(6)	0.886(1)	C(15)	-0.046(1)	0.132 5(7)	0.631(1)
O(5)	-0.077(1)	0.342 9(6)	0.626(1)	C(16)	-0.185(1)	0.137 7(8)	0.646(2)
O(6)	0.386(1)	0.457 6(6)	0.647(1)	C(17)	-0.258(2)	0.109 7(9)	0.768(2)
O(7)	0.508(1)	0.219 8(6)	0.058(1)	C(18)	-0.197(1)	0.077 8(8)	0.870(2)
O(8)	0.362 5(10)	0.434 9(6)	0.138(1)	C(19)	-0.060(1)	0.072 5(7)	0.860(1)
O(9)	0.672(1)	0.402 5(6)	0.483(1)	C(20)	0.014(1)	0.099 5(7)	0.738(1)
C(1)	0.484(2)	0.132 2(10)	0.368(2)	C(21)	-0.276(2)	0.050 0(10)	1.003(2)
C(2)	0.515(1)	0.252 4(8)	0.634(2)	C(22)	0.053(1)	0.319 0(7)	0.242(1)
C(3)	0.347(1)	0.103 2(9)	0.612(2)	C(23)	-0.046(1)	0.281 4(7)	0.114(1)
C(4)	0.231(1)	0.272 0(7)	0.764(1)	C(24)	-0.130(1)	0.323 7(8)	0.051(1)
C(5)	0.025(1)	0.324 6(8)	0.598(1)	C(25)	-0.118(1)	0.400 8(8)	0.111(1)
C(6)	0.318(1)	0.391 5(8)	0.605(1)	C(26)	-0.021(1)	0.438 9(8)	0.236(1)
C(7)	0.463(1)	0.254 6(8)	0.159(1)	C(27)	0.062(1)	0.398 1(7)	0.302(1)
C(8)	0.366(1)	0.386 7(8)	0.212(1)	C(28)	-0.210(2)	0.448 6(9)	0.040(2)

Additional material available from the Cambridge Crystallographic Data Centre comprises H-atom coordinates, thermal parameters and remaining bond parameters.

### Acknowledgements

We gratefully acknowledge the financial support from the Hong Kong Research Grants Council and the University of Hong Kong for this work. S. C. and W.-Y. W. thank the Croucher Foundation for financial support.

### References

- See, for example, R. B. King and C. W. Eavenson, *J. Organomet. Chem.*, 1972, **42**, C95; R. B. King and A. Efraty, *J. Am. Chem. Soc.*, 1972, **94**, 3021; R. B. King, I. Haiduc and C. W. Eavenson, *J. Am. Chem. Soc.*, 1973, **95**, 2508; R. D. Adams, J. E. Babin, M. Tasi and J. G. Wang, *Organometallics*, 1988, **7**, 755; D. Heineke and H. Vahrenkamp, *Organometallics*, 1990, **9**, 1697; J. F. Corrigan, S. Doherty, N. J. Taylor and A. J. Carty, *Organometallics*, 1992, **11**, 3160; 1993, **12**, 1365.
- E. L. Muettterties, T. N. Rhodin, E. Band, C. F. Brucker and W. R. Pretzer, *Chem. Rev.*, 1979, **79**, 91.
- E. L. Muettterties and J. Stein, *Chem. Rev.*, 1979, **79**, 479.
- L. R. Beanan, Z. A. Rahman and J. B. Keister, *Organometallics*, 1983, **2**, 1062 and refs. therein.
- N. Basescu, Z. X. Liu, D. Moses, A. J. Heeger, H. Naarmann and N. Theophilou, *Nature (London)*, 1987, **327**, 403.
- S. Chan, W. Y. Wong and W. T. Wong, *J. Organomet. Chem.*, 1994, **474**, C30.
- See, for example, B. F. G. Johnson, J. Lewis, J. Lunniss, D. Braga and F. Grepioni, *J. Organomet. Chem.*, 1991, **412**, 195; S. Aime, L. Milone, D. Osella and M. Valle, *J. Chem. Res.*, 1978, (S)77; (M)785; G. Gervasio, D. Osella and M. Valle, *Inorg. Chem.*, 1976, **15**, 1221; E. Boyar, A. J. Deeming, M. S. B. Felix, S. E. Kabir, T. Adatia, R. Bhusate, M. McPartlin and H. R. Powell, *J. Chem. Soc., Dalton Trans.*, 1989, **5**; A. J. Deeming, S. Hasso and M. Underhill, *J. Organomet. Chem.*, 1974, **80**, C53.
- See, for example, R. D. Adams, J. E. Babin, M. Tasi and J. G. Wang, *Organometallics*, 1988, **7**, 755; B. F. G. Johnson, R. Khattar, J. Lewis and P. R. Raithby, *J. Organomet. Chem.*, 1987, **335**, C17; R. D. Adams, I. Arafa, G. Chen, J. C. Lii and J. G. Wang, *Organometallics*, 1990, **9**, 2350; W. B. Fehlhammer and H. Stolzenberg, *Comprehensive Organometallic Chemistry*, eds. G. Wilkinson, F. G. A. Stone and E. Abel, Pergamon, Oxford, 1982, ch. 31.4; U. Riaz, M. D. Curtis, A. L. Rheingold and B. S. Haggerty, *Organometallics*, 1990, **9**, 2647.
- D. Braga, F. Grepioni, B. F. G. Johnson, J. Lewis and J. Lunniss, *J. Chem. Soc., Dalton Trans.*, 1991, 2223.
- J. T. Park, J. R. Shapley, M. R. Churchill and C. Bueno, *J. Am. Chem. Soc.*, 1983, **105**, 6182.
- D. Heineke and H. Vahrenkamp, *J. Organomet. Chem.*, 1993, **451**, 147.

- 12 S. Aime, L. Milone, E. Sappa and A. Tiripicchio, *J. Chem. Soc., Dalton Trans.*, 1977, 277.
- 13 V. Raverdino, S. Aime, L. Milone and E. Sappa, *Inorg. Chim. Acta*, 1978, **30**, 9.
- 14 M. Evans, M. Hursthouse, E. W. Randall, E. Rosenberg, L. Milone and M. Valle, *J. Chem. Soc., Chem. Commun.*, 1972, 545.
- 15 A. G. Orpen, *J. Chem. Soc., Dalton Trans.*, 1980, 2509.
- 16 J. B. Keister and L. R. Beanan, *Organometallics*, 1985, **4**, 1713.
- 17 J. W. Ziller, D. K. Bower, D. M. Dalton, J. B. Keister and M. R. Churchill, *Organometallics*, 1989, **8**, 492.
- 18 M. R. Churchill, L. A. Buttrey, J. B. Keister, J. W. Ziller, T. S. Janik and W. S. Striejewske, *Organometallics*, 1990, **9**, 766.
- 19 M. R. Churchill and B. G. DeBoer, *Inorg. Chem.*, 1977, **16**, 878.
- 20 R. D. Adams and W. Wu, *Organometallics*, 1993, **12**, 1243.
- 21 See, for example, G. Ferraris and G. Gervasio, *J. Chem. Soc., Dalton Trans.*, 1974, 1813; O. Gambino, R. P. Ferrari, M. Chinone and G. A. Vaglio, *Inorg. Chim. Acta*, 1975, **12**, 155; B. F. G. Johnson, R. Khattar, J. Lewis and P. R. Raithby, *J. Organomet. Chem.*, 1987, **335**, C17; O. Gambino, G. A. Vaglio, R. P. Ferrari and G. Cetini, *J. Organomet. Chem.*, 1971, **30**, 381.
- 22 M. R. Churchill and R. A. Lashewycz, *Inorg. Chem.*, 1978, **17**, 1291.
- 23 P. F. Jackson, B. F. G. Johnson, J. Lewis, P. R. Raithby and G. J. Will, *J. Chem. Soc., Chem. Commun.*, 1980, 1190.
- 24 E. O. Greaves, G. R. Knox and P. L. Pauson, *Chem. Commun.*, 1969, 1124.
- 25 A. J. Edwards, M. A. Gallop, B. F. G. Johnson, J. U. Kohler, J. Lewis and P. R. Raithby, *Angew. Chem., Int. Ed. Engl.*, 1994, **33**, 1093.
- 26 E. Sappa, A. M. M. Lanfredi, A. Tiripicchio, *Inorg. Chim. Acta*, 1980, **42**, 255.
- 27 G. Gervasio, E. Sappa, A. M. M. Lanfredi and A. Tiripicchio, *Inorg. Chim. Acta*, 1983, **68**, 171.
- 28 B. F. G. Johnson, R. Khattar, J. Lewis, P. R. Raithby and D. N. Smit, *J. Chem. Soc., Dalton Trans.*, 1988, 1421.
- 29 B. F. G. Johnson, J. W. Kelland, J. Lewis, A. L. Mann and P. R. Raithby, *J. Chem. Soc., Chem. Commun.*, 1980, 547.
- 30 M. R. Churchill, J. W. Ziller, J. R. Shapley and W. Y. Yeh, *J. Organomet. Chem.*, 1988, **353**, 103.
- 31 W. Y. Wong, S. Chan and W. T. Wong, *J. Organomet. Chem.*, 1995, in the press.
- 32 P. R. Raithby and M. J. Rosales, *Adv. Inorg. Chem. Radiochem.*, 1985, **29**, 169.
- 33 See, for example, R. C. Ryan, C. U. Pittman and J. P. O'Connor, *J. Am. Chem. Soc.*, 1977, **99**, 1986; C. U. Pittman and R. C. Ryan, *Chem. Technol.*, 1978, **8**, 170; B. Heil and L. Marko, *Chem. Ber.*, 1969, **102**, 2238; M. Valle, D. Osella and G. A. Vaglio, *Inorg. Chim. Acta*, 1976, **20**, 213; H. Kang, C. H. Mauldin, T. Cole, W. Slegeir, K. Cann and R. Pettit, *J. Am. Chem. Soc.*, 1977, **99**, 8323; R. M. Laine, *J. Am. Chem. Soc.*, 1978, **100**, 6451; R. Whyman, *Transition Metal Clusters*, ed. B. F. G. Johnson, Wiley, New York, 1980, p. 557.
- 34 R. B. Anderson, *The Fischer-Tropsch Synthesis*, Academic Press, London, 1984.
- 35 G. A. Somorjai, *Introduction to Surface Chemistry and Catalysis*, Wiley, New York, 1994.
- 36 J. G. McCarty and H. Wise, *J. Catal.*, 1979, **57**, 406.
- 37 J. S. Bradley, *Adv. Organomet. Chem.*, 1983, **22**, 1.
- 38 T. Dutton, B. F. G. Johnson, J. Lewis, S. M. Owen and P. R. Raithby, *J. Chem. Soc., Chem. Commun.*, 1988, 1423.
- 39 P. Mains, S. J. Fiske, S. E. Hull, L. Lessinger, G. Germain, J. P. Declercq and M. M. Woolfson, MULTAN 82, A System of Computer Programs, for the Automatic Solution of Crystal Structures, Universities of York and Louvain, 1991.
- 40 H. F. Fan, SAPI91, Structure Analysis Programs with Intelligent Control, Rigaku Corporation, Tokyo, Japan, 1991.
- 41 M. C. Burla, M. Camalli, G. Cascarano, C. Giacovazzo, G. Polidori, R. Spagna and D. Viterbo, *J. Appl. Crystallogr.*, 1989, **22**, 389.
- 42 A. C. T. North, D. C. Phillips and F. S. Mathews, *Acta Crystallogr., Sect. A*, 1968, **24**, 351.
- 43 SDP Structure Determination Package, Enraf-Nonius, Delft, 1985.
- 44 TEXSAN, Crystal Structure Analysis Package, Molecular Structure Corporation, 1985 and 1992.

Received 16th November 1994; Paper 4/07011I